THE EFFECT OF DISSIPATION ON SOLUTIONS OF THE GENERALIZED KORTEWEG-DE VRIES EQUATION

J. L. Bona[1,2] , V. A. Dougalis[3,4] , O. A. Karakashian[5] & W. R. McKinney[6]

Abstract. It was indicated in recent numerical simulations that the initial-value problem for the generalized Korteweg-de Vries equation is not globally well posed when the nonlinearity is strong enough. Indeed, even C^∞ -initial data that is spatially periodic is observed to form singularities in finite time. The generalized Korteweg-de Vries equations are Hamiltonian systems that feature a competition between nonlinear and dispersive effects. A natural question that comes to the fore in consequence of the observed singularity formation is whether or not the addition of a term modelling the effect of dissipation will eliminate singularities and so result in an initial-value problem that is globally well posed. It is the purpose of the present paper to study this question both analytically and numerically. Our concern will be mainly with the addition of a Burgers-type dissipative term because of its frequent appearance in practical modelling problems. Some commentary is also provided about the situations that obtain when other dissipative mechanisms are introduced. It seems that singularity formation persists in the presence of small amounts of dissipation, but ceases at a certain critical level whose general form is studied both numerically and analytically.

1. Introduction

The present paper is inspired by an earlier one of the same authors and aims to add considerably to the conclusions drawn therein. In the previous study (Bona *et al.* 1994), attention was given to the development and use of numerical approximations of solutions to the initial- and periodic-boundary-value problem for the generalized Korteweg-de Vries equation (GKdV equation henceforth)

$$u_t + u^p u_x + \varepsilon u_{xxx} = 0. \tag{1.1a}$$

Here, the dependent variable $u = u(x,t)$ is a 1-periodic, real-valued function of the spatial variable $x \in [0,1]$ and the temporal variable $t \geq 0$ which is prescribed at $t = 0$ by

$$u(x,0) = u_0(x) \tag{1.1b}$$

[1]Department of Mathematics, Penn State University, University Park, PA 16802 USA
[2]Applied Research Laboratory, Penn State University, University Park, PA 16802 USA
[3]Mathematics Department, National Technical University, Zographou, 15780 Athens, Greece
[4]Institute of Applied and Computational Mathematics, FORTH, Heraklion, Greece
[5]Department of Mathematics, University of Tennessee, Knoxville, TN 37996 USA
[6]Department of Mathematics, North Carolina State University, Raleigh, NC 27607 USA

for $0 \leq x \leq 1$. In (1.1a), ε is a fixed, positive number that is related to a generalization of the classical Stokes number of surface water-wave theory (see Albert & Bona 1991, Bona & Sciálom 1993) and p is a positive integer. Special consideration was given in our previous work to understanding the instability of the travelling-wave solutions of (1.1a) called solitary waves, and it transpired that this instability manifests itself in blow-up in finite time. More precisely, if $p \geq 4$ in (1.1a), then perturbations of solitary waves form a similarity structure under the evolution (1.1a) and this structure in turn blows up, leading to the inference that there is a point (x^*, t^*) such that $u(x,t) \longrightarrow +\infty$ as $(x,t) \longrightarrow (x^*, t^*)$. These earlier numerical simulations showed also that this special blow-up phenomenon has more scope than might be expected. A broad class of initial data u_0 has the property that, under the evolution (1.1a), the resulting solutions rapidly decompose into a finite number of pulses resembling solitary waves, the first and largest of which then becomes unstable, forms a similarity structure and blows up in finite time. As nearly as could be discerned from the numerical simulations, the process of singularity formation for general initial data u_0 was the same as that appearing in the instability of the solitary wave.

It is worth noting that the blow-up phenomenon just described subsists on both nonlinear and dispersive effects, and it can only occur if the nonlinearity overpowers the dispersion. Three facts support this conclusion. First, if $\varepsilon = 0$, so that dispersion is absent, there are large classes of initial data whose corresponding solutions form singularities in finite time, but it is the derivative that becomes unbounded, not the solution itself. Second, if $p < 4$, then smooth initial data u_0 lead to global solutions u of the initial-value problem (1.1), regardless of the size of the data (see Kato 1983, Albert *et al.* 1988). Finally, even for $p \geq 4$, if the initial data u_0 is reasonably smooth and small enough so that one expects nonlinear effects to be relatively insignificant, then the initial-value problem (1.1) still has global solutions (cf. Strauss 1974, Schechter 1978, Kato 1983).

The GKdV equations arise in modelling the propagation of small-amplitude, long waves in nonlinear dispersive media (see Benjamin *et al.* 1972, Benjamin 1974). The case $p = 1$

is the classical Korteweg-de Vries (KdV) equation about which much has been written in the last three decades, and which arises in a number of interesting physical situations (cf. Benjamin 1974, Jeffrey & Kakutani 1972, Scott *et al.* 1973). In real physical situations, dissipative effects are often as important as nonlinear and dispersive effects (see the experimental study of Bona *et al.* 1981) and this fact has given currency to the study of the Korteweg-de Vries-Burgers equation

$$u_t + uu_x - \delta u_{xx} + \varepsilon u_{xxx} = 0 \tag{1.2}$$

as a model that incorporates all three effects (see Grad & Hu 1967, Johnson 1970, Bona & Smith 1975, Bona *et al.* 1981, Bona & Schonbek 1985, Pego 1985, Amick *et al.* 1989, Bona *et al.* 1992). In (1.2), the parameter ε is as before and $\delta > 0$ is another parameter expressing the relative strength of dissipative to nonlinear effects.

A natural question arises as to whether dissipative effects in the form of a Burgers-type term, say, overcome the nonlinear-dispersive interaction that leads to blow-up. It is to this and related questions that the present work is directed. For the most part, attention is given to the initial-value problem

$$\begin{aligned} u_t + u^p u_x - \delta u_{xx} + \varepsilon u_{xxx} &= 0, \\ u(x,0) &= u_0(x), \end{aligned} \tag{1.3}$$

where $p \geq 4$, u_0 is a reasonably smooth, 1-periodic, real-valued function on the real line $\mathbb{R}$, and ε and δ are positive constants as indicated previously. It is straightforward to show that the initial-value problem (1.3) has unique solutions corresponding to reasonably smooth initial data, at least locally in time, by semigroup methods (Kato 1975, 1983) or by regularization techniques (Bona & Smith 1975).

It is also easy to ascertain that a solution of (1.3) defined locally in time has a global extension if it remains bounded in a suitable norm on bounded time intervals (see Kato 1983, Albert *et al.* 1988 or Bona *et al.* 1987). However, standard energy techniques seem unable to establish the *a priori* deduced bounds needed to guarantee global existence.

It will be shown below that for fixed $\varepsilon > 0$ and for any given initial datum u_0, there is a $\delta_c > 0$ such that if $\delta > \delta_c$, then the local solution of (1.3) emanating from u_0 has a global continuation as a smooth solution of the differential equation. This global result was motivated by the outcome of a series of numerical experiments simulating solutions of (1.3) which were designed to cast light on the effect of the dissipative term. Other interesting points are indicated by these numerical results which are described in the detailed outline of the paper to be presented now.

The plan of the paper is straightforward. Section 2 contains theoretical results appertaining to (1.3) and one of its near relatives wherein the dissipative term $-\delta u_{xx}$ is replaced by σu. We are able to establish in both cases that if the parameter δ or σ is sufficiently large relative to certain norms of the initial data u_0, then the solution u emanating from u_0 exists and is uniformly bounded over the entire temporal half-axis $[0, \infty)$. Moreover, the proofs lead to explicit formulas for an upper bound on the critical values δ_c and σ_c at least when u_0 is a perturbed solitary wave that would blow up in finite time in the absence of dissipation. When a solution is global in time, results about its decay to a quiescent state are also derived.

Section 3 contains a description of the numerical method used to integrate (1.3). As in our earlier study, the scheme is based on a Galerkin spatial discretization with periodic, cubic splines coupled with a time-stepping procedure which combines a two-stage Gauss-Legendre implicit Runge-Kutta method with a version of Newton's method for solving the system of nonlinear equations that arise at each time step. This basic scheme is augmented by adaptive mechanisms that adjust the temporal and local spatial grids in an effort to retain accuracy in the face of large values of the dependent variable.

Section 4 reports on numerical experiments carried out using a computer code derived from the numerical scheme described in Section 3. In Subsection 4a, computations show that solutions of (1.3) still blow up in finite time for $p = 5, 6$ or 7 provided the dissipative coefficient δ is small enough. The computed rates of blow-up and the structure of solutions

as they become singular are virtually identical to those observed for the non-dissipative problem in which $\delta = 0$. An analysis of the data presented shows the interesting conclusion that the theoretically derived forms for the critical values δ_c and σ_c coincide with those obtained in practice.

Subsection 4b records some data connected with the decay of solutions when the parameter δ is large enough to prevent blow-up. It is shown in Section 2 that in this circumstance solutions approach exponentially a constant equal to the mean value of u_0. The lapse rate in the exponential decay depends linearly on δ and tends to zero as δ tends to zero. The numerically obtained evidence supports the contention that for any p, the long-term behavior of global solutions is determined by the linearized form of the GKdV equation, a conclusion that agrees with Biler's sharp decay results for the case $p = 1$ (Biler 1984). Commentary is also offered about the transitory, oscillatory break-up of initial data that occurs at early stages in the evolution prior to the long-term, exponential asymptotics becoming dominant.

The paper concludes with a summary section that also features remarks on potentially interesting avenues for further research.

2. Theoretical Results

After a review of notational conventions, the principal theorem in our theoretical development is stated and proved. Several useful corollaries are then derived which act as a foil for some of the numerical simulations presented in Section 4.

Notation. In the sequel L_q, $1 \leq q < \infty$ will denote the collection of L-periodic functions which are q^{th}-power integrable over $[0, L]$ endowed with the norm

$$|f|_q = \left(\int_0^L |f(x)|^q \, dx \right)^{1/q},$$

with the usual modification if $q = \infty$. For $s \geq 0$, the space $H^s = H^s(0, L)$ is the Sobolev class of L-periodic functions which, along with their first s derivatives belong to L_2. The

usual norm on H^s is denoted by $\|\cdot\|_s$. The norm of $L_2 = H^0$ appears frequently and will be denoted $|\cdot|_2$ rather than $\|\cdot\|_0$; the associated inner product is the only Hilbert-space structure to intervene in the analysis and it is written simply as $(\cdot,\cdot)$. In Sections 3 and 4, we shall restrict attention to the case where $L = 1$. For the periodic problem, this simply amounts to a rescaling of the spatial variable x, and no loss of generality results from this presumption. However, in the present section, it will be convenient to leave L arbitrary for reasons that will become apparent shortly.

It deserves remark that while it is convenient to present analytical results first, early numerical results helped motivate the theory which in turn provided significant insights and guidance into later numerical experiments.

As an example, which sets the stage for Theorem 2.1, the reader may consult Figures 1a and 2 in Section 4 that depict the outcome of two numerical simulations of (1.2), both with $p = 5$, ε fixed and the same initial data. The difference between the two simulations lies with the value of the dissipative parameter δ; in Figure 1a, δ is rather small while in Figure 2 it is five times larger. As documented in detail in Subsection 4a, the smaller value of δ seems to allow the associated solution to form a singularity in finite time, whereas the larger value of δ appears to prevent the single-point blow-up observed in Figure 1a.

Armed with these, and other like results, for different values of p, the following theorem was conjectured and proved.

THEOREM 2.1. *Let u_0 be given initial data that is periodic of period $L > 0$ and suppose u_0 to lie in $H^s(0,L)$ for some $s \geq 2$. Let $\varepsilon, \delta > 0$ be given.*

(1) If $p < 4$, then there is a unique global solution u of (1.3) corresponding to the above specification of data and parameters, that lies in $C(0,T;H^s(0,L))$ for every $T > 0$. Moreover, $\|u(\cdot,t)\|_1$ is uniformly bounded in t.

(2) If $p \geq 4$, there is a $T_0 > 0$ depending on $\|u_0\|_1$ and a unique solution $u \in C(0,T_0;H^s(0,L))$ of (1.3) with initial data u_0. If $\|u_0\|_1$ is sufficiently small with respect to

δ, then T can be taken arbitrarily large, the solution is global, and $\|u(\cdot,t)\|_1$ is uniformly bounded for $t \in [0,+\infty)$.

In all the above cases, the solution u depends continuously on the initial data u_0 in that the mapping $u_0 \mapsto u$ is continuous from H^s to $C(0,T;H^s)$.

Remark. Part (1) and the local existence theory in Part (2) may be found more or less as stated in the literature (cf. Bona & Smith 1975, Kato 1975, 1983, Albert *et al.* 1988 Albert & Bona 1991). It deserves remark that the correspondence $u_0 \mapsto u$ has recently been investigated in more detail by Bourgain (1993) and Zhang (1993), with the outcome that values of s smaller than 2 can be accomodated and the correspondence, much more than being continuous, is analytic. Moreover, since $\delta > 0$, coarse data becomes smooth for $t > 0$. None of these subtle aspects are important in our analysis, however, so we pass over them in favor of the simpler description in Theorem 2.1.

Proof. Attention will be given only to the case $p \geq 4$. As mentioned above, a theory, local in time, of existence, uniqueness and continuous dependence for (1.3) may be concluded using standard semigroup theory, and the details are therefore omitted. The focus of attention here will be to provide *a priori* deduced bounds that allow the local theory to be continued indefinitely. Finer results from the local theory can be deduced, but for our purposes it will suffice to note that if the initial data u_0 lies in H^s for some $s \geq 2$, and if the solution u is bounded, at least on any interval of the form $[0,T]$ for finite $T > 0$, then the solution is global in time and lies in $C(0,T;H^s)$ for all finite T. This state of affairs can be ascertained from Kato's theory (Kato 1975, 1983, Albert *et al.* 1988) or from the estimates to be derived now.

Let u be a solution in $C(0,T;H^s)$ corresponding to initial data u_0 of the initial-value problem (1.3), where $s \geq 2$. Without loss of generality, we may suppose that s is large enough that the formal calculations to follow are straightforwardly justified. Because of the continuous dependence of the solution on the initial data, one simply regularizes the initial

data, makes the calculations with the associated smoother solutions, and after deriving the desired inequalities, then passes to the limit as the regularization disappears. So long as the inequalities in question do not involve derivatives higher than those appearing in the initial data, this procedure leads securely to the desired results.

We begin by multiplying the equation (1.2) by the solution u, integrating the result with respect to x over the period $[0, L]$ and with respect to t over the interval $[0, t_0]$, where $t_0 \leq T$. After suitable integrations by parts, and using periodicity to see that the boundary terms cancel, there appears the simple relation

$$|u(\cdot, t_0)|_2^2 + 2\delta \int_0^{t_0} |u_x(\cdot, t)|_2^2 \, dt = |u_0|_2^2. \tag{2.1}$$

(Throughout this proof, all the norms are computed with respect to the spatial region $[0, L]$.) It is deduced from this that $|u(\cdot, t)|_2$ is a decreasing function of time and that

$$\int_0^t |u_x(\cdot, t)|_2^2 \, dt$$

is bounded independently of t.

The next stage of the estimates is more complicated. As shown in Kato (1983) and Albert *et al.* (1988), all that is required in order to infer the boundedness of u in H^s on bounded time intervals, and thereby to deduce the conclusion of the theorem is to demonstrate that the L_∞-norm of the solution is bounded on bounded time intervals. For this, it suffices to show the H^1-norm of the solution is bounded on bounded time intervals. In fact, we shall show that the H^1-norm of solutions corresponding to initial data suitably small with respect to δ is bounded independently of t.

To this end, let $\overline{u}_0 = \frac{1}{L} \int_0^L u_0(x) dx$ be the average mass of the initial data. By integrating (1.2) with respect to x, one readily deduces from the spatial periodicity that for any $t > 0$ for which the solution exists on $[0, t]$, one has $\overline{u}(t) = \frac{1}{L} \int_0^L u(x, t) dx = \overline{u}_0$. (This is a reflection of conservation of mass in some applications of this class of equations to practical situations.)

Define a new dependent variable v by $v(x,t) = u(x,t) - \overline{u}_0$. Then the variable v has total mass zero and satisfies the initial-value problem

$$\begin{aligned} v_t + \frac{1}{p+1}\partial_x(v+\overline{u}_0)^{p+1} - \delta v_{xx} + \varepsilon v_{xxx} = 0, \\ v(x,0) = v_0(x) = u_0(x) - \overline{u}_0. \end{aligned} \tag{2.2}$$

Multiply the differential equation in (2.2) by v_{xx} and integrate over $[0,L]$ to obtain the following differential inequality:

$$\begin{aligned} \frac{1}{2}\frac{d}{dt}\int_0^L v_x^2 dx + \delta \int_0^L v_{xx}^2 dx &= \frac{1}{p+1}\int_0^L \partial_x(v+\overline{u}_0)^{p+1} v_{xx} dx \\ &= \frac{1}{p+1}\int_0^L \partial_x \left(\sum_{j=0}^{p+1} \binom{p+1}{j} v^{p+1-j}\, \overline{u}_0^j \right) v_{xx} dx \\ &= \frac{1}{p+1}\int_0^L \sum_{j=0}^{p-1} \binom{p+1}{j} (p+1-j) v^{p-j} v_x \overline{u}_0^j\, v_{xx} dx \\ &\le \frac{1}{p+1}\sum_{j=0}^{p-1} \binom{p+1}{j} (p+1-j)\, |\overline{u}_0|^j |v|_\infty^{p-j}\, |v_x|_2\, |v_{xx}|_2. \end{aligned} \tag{2.3}$$

It is elementary that if w is periodic with mean value equal to zero, then

$$|w|_\infty^2 \le |w|_2\, |w_x|_2, \qquad |w_x|_2^2 \le |w|_2\, |w_{xx}|_2, \tag{2.4}$$

and

$$|w|_2 \le \frac{L}{2\pi}\, |w_x|_2.$$

If we use the first two of these relations systematically in (2.3), we ascertain that the right-hand member of (2.3) may be bounded above as follows:

$$\begin{aligned} &\frac{1}{p+1}\sum_{j=0}^{p-1} \binom{p+1}{j} (p+1-j) |\overline{u}_0|^j |v|_2^{\frac{p-j}{2}}\, |v_x|_2^{\frac{p+2-j}{2}}\, |v_{xx}|_2 \\ \le \frac{1}{p+1} &\left[\sum_{j=0}^{p-2} \binom{p+1}{j} (p+1-j)\, |\overline{u}_0|^j |v|_2^{\frac{p+2-j}{2}}\, |v_x|_2^{\frac{p-2-j}{2}}\, |v_{xx}|_2^2 \right. \\ &\left. + 2\binom{p+1}{p-1} |\overline{u}_0|^{p-1} |v|_2^{1/2}\, |v_x|_2^{\frac{3}{2}}\, |v_{xx}|_2 \right]. \end{aligned} \tag{2.5}$$

The last summand on the right-hand side of (2.5) requires special treatment; using the second relation in (2.4), one sees that

$$|v|_2^{1/2}|v_x|_2^{3/2}|v_{xx}|_2 \le (L/2\pi)^{1/2}|v_x|_2^2|v_{xx}|_2$$
$$\le (L/2\pi)^{1/2}|v|_2|v_{xx}|_2^2.$$

Putting this together with (2.5) and (2.3) leads to the differential inequality

$$\frac{1}{2}\frac{d}{dt}|v_x(\cdot,t)|_2^2 + \delta\,|v_{xx}(\cdot,t)|_2^2 \le \theta|v_{xx}(\cdot,t)|_2^2, \tag{2.6}$$

where

$$\theta = \theta(|v|_2, |v_x|_2, |\overline{u}_0|) =$$
$$\frac{1}{p+1}\left[\sum_{j=0}^{p-2}\binom{p+1}{j}(p+1-j)\,|\overline{u}_0|^j|v|_2^{\frac{p+2-j}{2}}\,|v_x|_2^{\frac{p-2-j}{2}}\right.$$
$$\left. +2\binom{p+1}{p-1}(L/2\pi)^{1/2}\,|\overline{u}_0|^{p-1}|v|_2\right].$$

Note that since v has mean value zero, then

$$|u(\cdot,t)|_2^2 = L\,\overline{u}_0^2 + |v(\cdot,t)|_2^2$$

while (2.7)

$$|u_x(\cdot,t)|_2^2 = |v_x(\cdot,t)|_2^2$$

for all t for which the solution exists. In consequence of these inequalities, it suffices to show that $\|v(\cdot,t)\|_1$ is bounded, independently of t, in order that $\|u(\cdot,t)\|_1$ is bounded, independently of t.

The differential inequality (2.6) is employed to deduce a global bound on $\|v(\cdot,t)\|_1$. Notice that θ is monotone increasing as a function of its three arguments. Moreover,

because of (2.1), $|u(\cdot,t)|_2 \le |u_0|_2$ whence $|v(\cdot,t)|_2 \le |u(\cdot,t)|_2 \le |u_0|_2$ in view of (2.7). In consequence of these two inequalities, we see that

$$\begin{aligned}
\theta &\le \frac{1}{p+1}\sum_{j=0}^{p-2}\binom{p+1}{j}(p+1-j)\left(\frac{|u_0|_2}{L^{1/2}}\right)^j |u_0|_2^{\frac{p+2-j}{2}}\,|v_x|_2^{\frac{p-2-j}{2}} \\
&\quad + \frac{2}{p+1}\binom{p+1}{p-1}(L/2\pi)^{1/2}\left(\frac{|u_0|_2}{L^{1/2}}\right)^{p-1}|u_0|_2 \\
&\le |u_0|_2^{\frac{p+2}{2}}\left\{\sum_{j=0}^{p-3}\binom{p+1}{j}\frac{p+1-j}{p+1}\left(\frac{|u_0|_2}{L}\right)^{j/2}|v_x|_2^{\frac{p-2-j}{2}}\right. \\
&\quad \left. + \left[\frac{3}{p+1}\binom{p+1}{p-2} + \frac{(2\pi^{-1})^{1/2}}{p+1}\binom{p+1}{p-1}\right]\left(\frac{|u_0|_2}{L}\right)^{\frac{p-2}{2}}\right\} \\
&\le \lambda_p |u_0|_2^{\frac{p+2}{2}}\sum_{j=0}^{p-2}\binom{p-2}{j}\left(\frac{|u_0|_2}{L}\right)^{j/2}|v_x|^{\frac{p-2-j}{2}} \\
&\le \lambda_p |u_0|_2^{\frac{p+2}{2}}\left(\frac{|u_0|_2^{1/2}}{L^{1/2}} + |v_x|_2^{1/2}\right)^{p-2} = \overline{\theta}(|u_0|_2, |v_x|_2),
\end{aligned} \tag{2.8}$$

for some constant λ_p depending only on p. If one rewrites (2.6) as

$$\frac{1}{2}\frac{d}{dt}|v_x(\cdot,t)|_2^2 + (\delta - \overline{\theta})|v_{xx}(\cdot,t)|_2^2 \le 0,$$

then it becomes clear that as soon as $\overline{\theta} \le \delta$, $|v_x(\cdot,t)|_2$ becomes monotone decreasing. In this range, $\overline{\theta}$ is also decreasing, and consequently if for some t_0 we find that $\overline{\theta} \le \delta$, then for all $t \ge t_0$ the same inequality holds. In particular, if at $t = 0$ it is the case that $\overline{\theta}(|u_0|_2, |v_{0x}|_2) = \overline{\theta}(|u_0|_2, |u_{0x}|_2) \le \delta$, then for all $t \ge 0$, $|v_x(\cdot,t)|_2 \le |u_{0x}|_2$, and so $\|v\|_1$ is seen to be bounded, independently of t.

Referring back to (2.8), if

$$\lambda_p |u_0|_2^{\frac{p+2}{2}}\left(\frac{1}{L^{1/2}}|u_0|_2^{1/2} + |u_{0x}|_2^{1/2}\right)^{p-2} \le \delta, \tag{2.9}$$

then $\|v(\cdot,t)\|_1$ is bounded, independently of t.

The theorem is thus established. □

Several interesting consequences can be drawn from this theorem and its proof. First, by letting the period L tend to $+\infty$, a result pertaining to the pure initial-value problem emerges. (The integrals in the norms mentioned in the following Corollary refer to the entire real axis $\mathbb{R}$.)

COROLLARY 2.2. *Let $u_0 \in H^s(\mathbb{R})$ for some $s \geq 2$ and let u be the corresponding solution of equation (1.2) for $x \in \mathbb{R}$ and $t > 0$ with parameters $\varepsilon, \delta > 0$ and $p \geq 4$. There is a constant $\mu = \mu_p$ depending only on p such that if*

$$|u_0|_2^{\frac{p+2}{2}} \, |u_{0x}|_2^{\frac{p-2}{2}} \leq \mu_p \delta, \tag{2.10}$$

then the solution lies in $C(0,T;H^s)$ for all $T > 0$ and $\|u(\cdot,t)\|_1 \leq \|u_0\|_1$ for all $t \geq 0$.

An interesting point arises relative to the inequality (2.10). It appears that this inequality is sharp in a certain way to be explained now. Consider the situation in which the initial data $u_0(x) = A\psi(Kx)$ for $x \in \mathbb{R}$, where A and K are positive constants. Then $|u_0|_2 = A|\psi|_2/K^{1/2}$ and $|u_{0x}|_2 = AK^{1/2}|\psi_x|_2$. Viewing ψ as fixed, but A, K as variable, we observe that inequality (2.10) becomes

$$\frac{A^p}{K} \leq \mu\delta \tag{2.11}$$

for a constant μ depending on p and norms of ψ. Of especial interest are the traveling-wave solutions of (1.1a) called solitary waves. These have the explicit form

$$u_s(x,t) = \mathrm{A}\mathrm{sech}^{2/p}[K(x - x_0) - \omega t] \tag{2.12a}$$

for any x_0, where the parameter K governing the spread of the solution and the speed of propagation ω are defined in terms of the amplitude A by

$$K = \left(\frac{p^2 A^p}{2\varepsilon(p+1)(p+2)}\right)^{1/2}, \quad \omega = \frac{2KA^p}{(p+1)(p+2)}. \tag{2.12b}$$

If the initial data u_0 lies close to a solitary-wave solution $u_s(\cdot,0)$ as defined above, then (2.11) becomes

$$\mu\delta \geq \frac{A^p}{\left(\frac{p^2A^p}{2\varepsilon(p+1)(p+2)}\right)^{1/2}} = d_pA^{p/2}\varepsilon^{1/2},$$

or what is the same,

$$\Delta = \frac{\delta^2}{\varepsilon A^p} \geq C_p, \tag{2.13}$$

where C_p is a constant depending on p and on the L_2-norms of $\mathrm{sech}^{2/p}(x)$ and its first derivative, and so in fact depends only on p.

As mentioned earlier, if $p \geq 4$, the solitary wave solutions of (1.2) with $\delta = 0$ are unstable (Bona *et al.* 1987, Pego & Weinstein 1992), and small perturbations were seen to lead to blow up in finite time (Bona *et al.* 1986, 1994). Consider now a situation where $\varepsilon > 0$ and $p \geq 5$ are fixed and initial data is specified to be $u_0(x) = \lambda u_s(x,0)$ where u_s is the solitary-wave solution in (2.12a) and λ is slightly greater than one, (e.g. $\lambda = 1.01$ as in §5 of Bona *et al.* 1994). With $\delta = 0$ and this initial data, the numerical approximation of the resulting solution of (1.2) indicates that it forms a singularity in finite time. Theorem 2.1 shows that for δ sufficiently large, the solution of (1.2) emanating from this type of initial data is uniformly bounded in t. One therefore expects a critical value δ_c of the dissipative parameter δ which defines the boundary between blow-up and global existence. From the condition in (2.13), it is known that $\delta_c^2 < C_p\varepsilon A^p$.

In Subsection 4a, an approximation of $\delta_c = \delta_c(A,\varepsilon)$ will be determined by making sequences of runs where u_0 is fixed as above and δ is varied systematically. It transpires that the combination denoted Δ in (2.13) is central to determining whether or not one has blow-up, at least for these perturbed solitary waves. It is a little unusual that the relatively crude energy estimates leading to the conclusion enunciated in (2.10) has this sharp aspect.

A final point that presents itself as a consequence of Theorem 2.1 is the decay of solutions to a quiescent state.

COROLLARY 2.3. *If u is a solution of the initial- and periodic-boundary-value problem (1.3) with $\delta > 0$ corresponding to initial data $u_0 \in H^s(0,L)$, then $|u(\cdot,t) - \overline{u}_0|_2 \leq e^{-\delta(\frac{2\pi}{L})^2 t}|u_0 - \overline{u}_0|_2$ for all t for which the solution exists. If u_0 satisfies condition (2.9) relative to δ, then $|u_x|_2$ also decays exponentially, as does $|\partial_x^j u|_2$ for all $j \leq s$.*

Proof. First, consider again the differential equation (2.2) satisfied by $v = u - \overline{u}_0$ and write it in the form

$$v_t + (v + \overline{u}_0)^p v_x + \varepsilon v_{xxx} - \delta v_{xx} = 0.$$

Multiply this by v and integrate the result over the period $[0, L]$ to reach the differential relation

$$\frac{1}{2}\frac{d}{dt}\int_0^L v^2 dx + \delta \int_0^L v_x^2 dx = 0.$$

Making use of (2.4) then implies that

$$\frac{d}{dt}\int_0^L v^2 dx + 2\delta\left(\frac{2\pi}{L}\right)^2 \int_0^L v^2 dx \leq 0,$$

whence $|v(\cdot,t)|_2 \leq |v(\cdot,0)|_2 e^{-\delta(\frac{2\pi}{L})^2 t}$ or what is the same, $|u(\cdot,t) - \overline{u}_0|_2 = O(e^{-\delta(\frac{2\pi}{L})^2 t})$ as $t \to +\infty$. Notice that this result is independent of p and the size of the data.

Now suppose the initial data u_0 satisfies the condition in (2.9). Since the L_2-norm of v is strictly decreasing and the H^1-semi-norm $|v_x|_2$ is non-increasing, it follows that for $t > 0$, $\theta = \theta(|v|_2, |v_x|_2, \overline{u}_0) < \delta$. Upon applying (2.4) to $|v_{xx}(\cdot,t)|_2$ in (2.6) we obtain that

$$\frac{1}{2}\frac{d}{dt}|v_x(\cdot,t)|_2^2 + (\delta - \theta)\left(\frac{2\pi}{L}\right)^2 |v_x(\cdot,t)|_2^2 \leq 0,$$

from which it is deduced that

$$|v_x(\cdot,t)|_2 \leq |v_x(\cdot,0)|_2 \exp\left[\left(\frac{2\pi}{L}\right)^2 \int_0^t (\theta - \delta) ds\right].$$

Thus $|v_x(\cdot,t)|_2$ is seen to be exponentially decreasing to zero, and since by (2.8) $\theta(t) \leq \overline{\theta} \leq \delta$, the asymptotic form of this decay is $O(e^{(\overline{\theta}-\delta)(\frac{2\pi}{L})^2 t})$ as $t \to +\infty$.

Similar considerations apply to higher-order semi-norms. We pass over the details. □

Remarks.

(i) Biler (1984) has obtained detailed decay estimates for periodic solutions in the case $p < 2$. See subsection 4b below for more commentary on his work.

(ii) This result is in marked contrast to the behavior of global solutions of the *pure* initial-value problem for (1.2) corresponding to initial data $u_0 \in H^s(\mathbb{R})$, $s \geq 2$. Such solutions are expected to decay to zero as $t \to +\infty$. However, the rate of decay is algebraic in t as witnessed by the results of Amick *et al.* (1989), where for $p = 1$ it was shown that

$$\int_{-\infty}^{\infty} u^2(x,t)dx = O\left(t^{-1/2}\right)$$

and that this rate was sharp in general. (See also the results of Bona & Luo 1993, Bona, Promislow & Wayne 1994, Dix 1992, and Zhang 1994 for $p \geq 2$.)

Dissipative mechanisms other than the Burgers-type appearing in (1.2) arise in practice. One particularly appealing dissipative mechanism is a simple, zero$^{\text{th}}$-order term corresponding to the initial-value problem

$$u_t + u^p u_x + \varepsilon u_{xxx} + \sigma u = 0, \tag{2.14}$$
$$u(x,0) = u_0(x),$$

where $\sigma > 0$. A theory entirely similar to that worked out for the initial-value problem (1.3) applies to (2.14). As there are some interesting mathematical points that arise, and because it ties in with some of the numerical simulations in Section 4, a sketch of the theory for (2.14) is provided.

THEOREM 2.4. *Let u_0 be given initial data that is periodic of period L and suppose u_0 to lie in $H^s(0,L)$ for some $s \geq 2$. Let $\varepsilon > 0$ and $\sigma \geq 0$ be given.*

(1) If $p < 4$, then there is a unique global solution u of (2.14) corresponding to the above specification of data and parameters which is periodic in x of period L that lies in $C(0,T;H^s)$ for every $T > 0$. Moreover, $\|u(\cdot,t)\|_1$ is uniformly bounded for $t \in [0,\infty)$.

(2) If $p \geq 4$, there is a $T_0 > 0$ depending on $\|u_0\|_1$ and a unique periodic solution $u \in C(0,T_0;H^s)$ of (2.14) with initial data u_0. If σ is sufficiently large with respect to $\|u_0\|_2$, then T_0 can be taken arbitrarily large, the solution u is global, and $\|u(\cdot,t)\|_1$ is uniformly bounded for $t \in [0,\infty)$.

In all the above cases, the mapping $u_0 \mapsto u$ is continuous from H^s to $C(0,T;H^s)$.

Proof. As in Theorem 2.1, attention is concentrated on the case $p \geq 4$. The case $p < 4$ is essentially contained in the existing literature, and the local well-posedness theory for $p \geq 4$ is a straightforward application of nonlinear semigroup theory. As before, the crux of the matter is an *a priori* deduced, L_∞-bound on u, and it suffices for this to show the H^2-norm is bounded, at least on bounded time intervals.

The analog of (2.1) is

$$|u(\cdot,t)|_2^2 + 2\sigma \int_0^t |u(\cdot,s)|_2^2 ds = |u_0|_2^2, \tag{2.15}$$

from which one deduces immediately that

$$|u(\cdot,t)|_2 = e^{-\sigma t}|u_0|_2. \tag{2.16}$$

The next step, if one were following the line of argument in Theorem 2.1, would be to subtract the mean value, multiply the resulting equation by v_{xx}, where $v = u - \overline{u}_0$, and integrate over $[0,L]$. This does not appear to be effective in the present case. Indeed, solutions of (2.14) have exponentially decaying rather than constant mean values. However, multiplying equation (2.14) by u_{xxxx} and integrating over $[0,L]$ is useful; after suitable

integrations by parts, this procedure leads to

$$\begin{aligned}\frac{1}{2}\frac{d}{dt}\int_0^L u_{xx}^2 dx + \sigma\int_0^L u_{xx}^2\,dx &= \int_0^L (u^p u_{xx} + pu^{p-1}u_x^2)u_{xxx}dx \\ &= -\frac{5p}{2}\int_0^L u^{p-1}u_x u_{xx}^2 dx - p(p-1)\int_0^L u^{p-2}u_x^3 u_{xx}\,dx \\ &\le \frac{5p}{2}|u|_\infty^{p-1}|u_x|_\infty|u_{xx}|_2^2 + p(p-1)|u|_\infty^{p-2}|u_x|_\infty^2|u_x|_2|u_{xx}|_2.\end{aligned} \tag{2.17}$$

Making systematic use of (2.4) for the zero-mean, periodic function u_x, together with the elementary inequality

$$|u|_\infty^2 \le \frac{1}{L}|u|_2^2 + 2|u|_2|u_x|_2, \tag{2.18}$$

it is deduced from (2.17) that

$$\frac{1}{2}\frac{d}{dt}|u_{xx}(\cdot,t)|_2^2 + (\sigma - \Omega)|u_{xx}(\cdot,t)|_2^2 \le 0, \tag{2.19}$$

where

$$\begin{aligned}\Omega = \Omega(|u|_2,|u_{xx}|_2) = \frac{5p}{2}\left(\frac{1}{L}|u|_2^2 + 2|u|_2^{3/2}|u_{xx}|_2^{1/2}\right)^{\frac{p-1}{2}}|u|_2^{1/4}|u_{xx}|_2^{3/4} \\ +p(p-1)\left(\frac{1}{L}|u|_2^2 + 2|u|_2^{3/2}|u_{xx}|_2^{1/2}\right)^{\frac{p-2}{2}}|u|_2|u_{xx}|_2.\end{aligned}$$

The function Ω is an increasing function of both its arguments. According to (2.16), $|u(\cdot,t)|_2$ is a decreasing function of $t \ge 0$. Hence if $\Omega|_{t=0} \le \sigma$, then $|u_{xx}(\cdot,t)|_2$ is non-increasing for $t \ge 0$. In particular, if

$$\Omega\left(|u_0|_2,|u_{0_{xx}}|_2\right) \le \sigma, \tag{2.20}$$

then the H^2-semi-norm $|u_{xx}(\cdot,t)|_2$ is bounded by its value at $t = 0$.

This concludes the proof of the theorem. □

COROLLARY 2.5. *Let $u_0 \in H^s(\mathbb{R})$ for some $s \ge 2$ and let u be the corresponding solution of the initial-value problem (2.14) with parameters $\varepsilon, \sigma > 0$ and $p \ge 4$. There is a constant $\nu = \nu_p$ depending only on p such that if*

$$|u_0|_2^{\frac{3p-2}{4}}|u_{0_{xx}}|_2^{\frac{p+2}{4}} \le \nu_p\sigma, \tag{2.21}$$

then $\|u(\cdot,t)\|_2$ *is uniformly bounded for all* $t \geq 0$.

Proof. Simply take the limit as $L \to +\infty$ in (2.20). □

Consider again the situation where $u_0(x) = A\psi(Kx)$ for some positive constants A and K. In this case, (2.21) amounts to the inequality

$$A^p K \leq \nu\sigma, \tag{2.22}$$

where ν is a constant depending on p, $|\psi|_2$, and $|\psi_{xx}|_2$. In particular, if $u_0 = \lambda u_s(x,0)$ is the perturbed solitary wave discussed earlier, then our theory implies that the solution emanating therefrom will exist globally in time provided

$$\Sigma = \frac{\sigma^{2/3}\mathcal{E}^{1/3}}{A^p} \geq C_p', \tag{2.23}$$

where C_p' is a constant depending only on p.

Just as for the initial-value problem (1.3) with $\delta > 0$, solutions of (2.14) that satisfy the initial restriction (2.20), decay to zero exponentially in t. This is already established for the L_2-norm, and for data respecting (2.20), the differential inequality (2.19) implies it for the H^2-semi-norm. Other semi-norms also decay exponentially. Note that in this case, the exponential decay rates are still valid in the limit as $L \to +\infty$ applicable to initial data in $H^s(\mathbb{R})$.

The theory propounded in this section will provide a framework for the numerical simulations of (1.3) and (2.14) reported in Section 4. In the next section, a careful description and associated benchmarks of our numerical schemes are provided.

3. The Numerical Method

After a brief review of preliminaries about splines and Runge-Kutta methods, the numerical technique used to approximate solutions of (1.3) and (2.14) is presented. Throughout this section and the next, the spatial period L will be normalized to the value 1.

The numerical scheme is a straightforward adaptation of one of the fully discrete Galerkin methods for (1.1) that was described in detail and analyzed in Bona *et al.* (1994). This scheme will be briefly reviewed below. We shall study its application to the initial- and periodic-boundary-value problem (1.3). Entirely analogous considerations apply when the scheme is used to solve the problem (2.14).

Let $r \geqq 3$ be an integer and $S_h = S_h^r$ be the N-dimensional vector space of 1-periodic smooth splines of order r (piecewise polynomials of degree $r-1$) on $[0,1]$ with uniform mesh length $h = 1/N$, where N is a positive integer. As usual, the standard semi-discretization of (1.2) in the space S_h is then defined to be the differentiable map $u_h : [0,T] \to S_h$ satisfying

$$(u_{ht} + u_h^p u_{hx}, \chi) - \varepsilon(u_{hxx}, \chi_x) + \delta(u_{hx}, \chi_x) = 0 \tag{3.1a}$$

for all $\chi \in S_h$ and $0 \leq t \leq T$, which is such that

$$u_h(0) = \Pi_h u_0. \tag{3.1b}$$

Here $\Pi_h u_0$ is any of several approximations of u_0 in S_h (for example, L_2-projection, interpolant, etc.) that satisfy an estimate of the form

$$|\Pi_h u_0 - u_0|_2 \leq c h^r \|u_0\|_r \tag{3.2}$$

for $u_0 \in H^r$, and where c is a constant independent of u_0 and h. (Constants independent of the discretization parameters will frequently occur in the sequel and will be denoted by c, C, etc.) For smooth, periodic initial data u_0 for which (3.2) holds, and assuming that the associated solution $u(x,t)$ of (1.3) is sufficiently smooth on $[0,T]$, it may be proved, following the analysis in Baker *et al.* (1983) that there is a constant $c = c(u)$ depending on the solution u, but not on the discretization parameter h, for which

$$\max_{0 \leq t \leq T} |u_h - u|_2 \leq c(u)\, h^r. \tag{3.3}$$

Upon choosing a basis for S_h and representing u_h in terms of this basis, the problem (3.1) is seen to be an initial-value problem for a system of ordinary differential equations which may be written compactly in the form

$$\begin{aligned} u_{ht} &= F(u_h)\ ,\ 0 \le t \le T, \\ u_h(0) &= \Pi_h\, u_0, \end{aligned} \tag{3.4}$$

where $F : S_h \longrightarrow S_h$ is defined by

$$(F(v), \chi) = -(v^p\, v_x, \chi) + (\varepsilon v_{xx} - \delta v_x, \chi_x) \tag{3.5}$$

for all $\chi \in S_h$. Having recognized (3.1) as the initial-value problem (3.4), an appropriate numerical method for the approximation of systems of ordinary differential equations leads to a fully discrete approximation to (1.3). In our companion paper on the non-dissipative case, use was made of the family of implicit Runge-Kutta methods of Gauss-Legendre type. These were found to possess favourable accuracy and stability properties when applied to (1.1). They can be extended in a straightforward way to the dissipative case at hand. In particular, the fact that these methods don't generate artificial damping is very helpful when small values of ν or σ are in question. For simplicity, consideration is given here only to the two-stage member of the Gauss-Legendre family. Let k be the time step (considered constant for the moment) and let $t_n = nk$, $n = 0, 1, 2, \ldots, J$, where J is some positive integer such that $Jk = T$. For each integer $n \in [0, J]$, we seek a function $U^n \in S_h$, with

$$U^0 = \Pi_h\, u_0 \tag{3.6}$$

and which approximates $u_n = u(\cdot, t_n)$, where $u(x,t)$ is the solution of (1.3). For $n = 0, 1, 2, \ldots, J-1$ the approximation U^{n+1} is constructed from U^n through two intermediate stages $U^{n,1}$ and $U^{n,2}$ in S_h that are solutions of the system of nonlinear equations

$$U^{n,i} = U^n + k \sum_{j=1}^{2} a_{ij}\, F(U^{n,j}), \qquad i = 1, 2\ , \tag{3.7a}$$

by the formula

$$U^{n+1} = U^n + k \sum_{j=1}^{2} b_j \, F(U^{n,j}), \tag{3.7b}$$

where the 2×2 matrix $A = (a_{ij})$ and the 2-vector $b = (b_1, b_2)^T$ that define the two-stage Gauss-Legendre method are given in the following tableau:

$$\begin{array}{cc|cc} a_{11} & a_{12} & \frac{1}{4} & \frac{1}{4} - \frac{1}{2\sqrt{3}} \\ a_{21} & a_{22} & \frac{1}{4} + \frac{1}{2\sqrt{3}} & \frac{1}{4} \\ \hline b_1 & b_2 & \frac{1}{2} & \frac{1}{2} \end{array} \quad .$$

In view of Lemma 3.2 of Bona *et al.* (1994), it is straightforward to generalize Proposition 3.1 of this reference to include the system under consideration here and thereby prove that for any given $U^n \in S_h$, there are elements $U^{n,1}$, $U^{n,2}$ of S_h that satisfy (3.7a). The scheme that then assigns to U^n the function U^{n+1} defined by (3.7b) is stable in L_2, which is to say that

$$|U^n|_2 \leq |U^0|_2 \quad \text{for } 1 \leq n \leq J. \tag{3.8}$$

The latter property follows from the well known conservative nature of the Gauss-Legendre implicit Runge-Kutta schemes implied by the fact that $b_i a_{ij} + b_j a_{ji} - b_i b_j = 0$ for all the relevant i, j. The fact that the time-stepping scheme is conservative means that $|U^n|_2 = |U^0|_2$ for $n = 1, \ldots, J$ in the non-dissipative case $\delta = 0$ since then $(F(v), v) = 0$ for all $v \, \varepsilon \, S_h$, whereas the inequality (3.8) holds when $\delta > 0$ since then $(F(v), v) \leq 0$ for all $v \, \varepsilon \, S_h$. It deserves remark that the use of a conservative time-stepping scheme to approximate solutions of a dissipative partial differential equation seemed to work very well in the numerical experiments to be reported later.

The following remarks are meant to summarize the convergence theory pertaining to the scheme just outlined. The theoretical analysis of this scheme for (1.3) with $\delta > 0$ follows in detail that already derived for the initial-value problem (1.1) with $\delta = 0$ in Bona

et al. (1994). Adapting the convergence proof contained in the last-cited reference leads immediately to the conclusion that, provided the solution is smooth enough on the time interval $[0,T]$ and k/h is sufficiently small, there is a unique solution U^n of (3.7) and it satisfies the optimal-order L_2-error estimate

$$\max_{0\le n\le J} |U^n - u(\cdot,t^n)|_2 \le c(k^4 + h^r). \tag{3.9}$$

Analogous estimates may be established for higher-order accurate Runge-Kutta time-stepping methods following the arguments in Karakashian & McKinney (1990). In the case of a q-stage Gauss-Legendre method with the same hypotheses about smoothness and k/h, (3.8) holds and (3.9) generalizes to the optimal-order L_2-estimate

$$\max_{0\le n\le J} |U^n - u(\cdot,t^n)|_2 \le c(k^{2q} + h^r).$$

It is well known that the temporal rate $2q$ obtained for the Gauss-Legendre method is the best that can be achieved by a q-stage Runge-Kutta method.

A word is appropriate about the numerical linear algebra involved in the implementation of the scheme described above. At each time step the $2\dim S_h \times 2\dim S_h$ nonlinear system represented in (3.7a) is solved by a doubly iterative scheme based on Newton's method. The work is organized in such a way that each time step only requires the solution of a small number of sparse, $\dim S_h \times \dim S_h$ complex linear systems with the same coefficient matrix. The details of the construction and implementation of this solver are virtually the same as those used earlier in the non-dissipative case described in Section 4 of Bona *et al.* (1994). In the numerical experiments whose outcome is presented here, use was made of only the simplest iterative scheme considered in the last-cited reference, namely the one corresponding to one "outer" (Newton) and two "inner" iterations at each time step; this scheme requires solving only two sparse complex systems of size $\dim S_h \times \dim S_h$ per time step. We pass over the details since they are adequately covered in the previous work. For a theoretical analysis of the approximation of solutions of nonlinear systems such as (3.7a) by Newton's method, see Karakashian & McKinney (1994).

It transpires that some of the solutions whose approximation is of interest feature very rapid spatial and temporal changes. To keep track of the solution in such circumstances, it proved necessary to introduce adaptive mechanisms into the numerical procedure. These mechanisms took two distinct forms. First, a criterion was designed to refine the temporal step size as the solution began to evolve rapidly, and then a procedure was developed to cut the spatial meshlength in a neighborhood of points where large values of the dependent variable are detected. The experiments reported here were all performed using a computer code that featured both of these developments. Their implementation is presented and discussed in Section 5 of Bona *et al.* (1994). It is geared toward approximating solutions that are developing a single peak that apparently becomes infinitely high at a finite time t^* at a well-defined point x^*. The spatial refinement is controlled by making use of a local version of the inverse $L_\infty - L_2$ inequality satisfied by members of S_h, and the temporal step is defined by reference to the local, temporal variation of the quantity

$$I_3(v) = \int_0^1 \left[v^{p+2}(x) - \varepsilon \frac{(p+1)(p+2)}{2} v_x^2(x) \right] dx. \tag{3.10}$$

More precisely, the computer code looks at the variation of $I_3(U^n)$ with n and cuts the time step when a normalized version of this quantity's change exceeds a specified tolerance. The functional I_3 came to the fore in the earlier work on the GKdV equation (1.1) because I_3 is an exact invariant of this evolution. That is, if $u = u(x,t)$ is an H^1-solution of (1.1), then $I_3(u(\cdot,t))$ is time independent. Although I_3 is no longer an invariant of the evolution generated by (1.2) when $\delta > 0$, its variation was still found to generate an effective criterion for keeping errors under control by refining the temporal discretization.

4. Numerical Experiments

The scheme just presented was used by Bona *et al.* (1994) in a detailed study of the initial-value problem for equation (1.1). As mentioned already, considerable attention was paid to issues surrounding the solitary-wave solutions written in (2.12). Although the

function $u_s(x,t)$ in (2.12a) is an exact solution of (1.1) when this equation is posed on the entire real line, one may use it to define a solution on $[0,1]$, say, with periodic boundary conditions imposed at the endpoints, as discussed in detail in Bona (1981). If A/ε is large, then u_s decays very rapidly away from its peak value. Hence if at $t = 0$ the peak is centered at the midpoint of the spatial interval ($x_0 = 1/2$ in (2.12a)), then to machine accuracy it defines initial data supported in $[0,1]$. Consequently, it may be extended to define periodic initial data thusly,

$$\tilde{u}_0(x) = \sum_{j=-\infty}^{\infty} u_s(x+j,0) \tag{4.1a}$$

and this data used to determine a spatially periodic solution of (1.2), say. As shown in Bona (1981), the periodic solution of (1.1a) emanating from $\tilde{u}_0$ above is, to very good approximation over relatively long time scales, given by

$$u(x,t) = \sum_{j=-\infty}^{\infty} u_s(x+j,t). \tag{4.1b}$$

The same remarks are valid for any initial data that decays rapidly to zero outside a finite region of space, although the longer the spatial period $[0,L]$, say, the longer the time scale over which the solution of the periodic initial-value problem is well approximated by (4.1b).

It is known from earlier theory (see Bona *et al.* 1987) that the solitary-wave solutions u_s in (2.12) are orbitally stable for $p < 4$ and unstable if $p \geq 4$. Also, while (1.1) is always locally well posed in reasonable function classes, it is known to be globally well posed for initial data unrestricted in size only when $p < 4$, (see Kato 1979, 1983, or Schechter 1978). Two natural questions arise from these theoretical considerations. First, what happens when an unstable solitary wave is perturbed? Second, is (1.1) globally well posed if $p \geq 4$? The numerical simulations in Bona *et al.* (1986) and Bona *et al.* (1994) indicate the answers to these two questions are related. The conclusions to which reference was just made were based on the outcome of numerical experiments conducted with the fully discrete, adaptive scheme presented in the previous section. It appears that the instability of the solitary-wave solution manifests itself in a transformation to a similarity solution

that goes on to develop a single-point blow-up in finite time. That is, there is a point $(x^*, t^*) \in [0,1] \times (0,\infty)$ such that $|u(x,t)| \to +\infty$ as $(x,t) \to (x^*, t^*)$, $t < t^*$. A detailed analysis of a considerable collection of numerical simulations support the more precise conjecture that the similarity solution corresponding to the blow-up has the form

$$u(x,t) = \frac{1}{(t^* - t)^{2/3p}} \chi\left(\frac{x^* - x}{(t^* - t)^{1/3}}\right) + \text{ bounded terms}, \tag{4.2}$$

where χ is a smooth, bounded function. These tentative conclusions in turn yield a negative answer to the question of whether or not the initial-value problem (1.3) is globally well posed for $p \geq 4$. Further experimentation showed that more general classes of initial data rapidly decomposed into profiles resembling a sequence of solitary waves, the largest of which loses stability and evolves into a similarity solution of the type indicated in (4.2) and thus proceeds to form a singularity in finite time.

4A. Blow-up for Small Dissipation

It is the aim in this section to understand how the results just reviewed are modified by the addition of a Burgers-type dissipative term as in equation (1.2) with small $\delta > 0$. As was seen in Section 2, for δ sufficiently large, the solution of the initial- and periodic-boundary-value problem (1.3) exists globally in time and decays to the mean of the initial data exponentially. However, if one sets as initial data a perturbed solitary wave that apparently blows up when $\delta = 0$, the numerical experiments indicate that for δ below a critical value δ_c, the resulting solution of (1.2) seems also to blow up. Moreover, the various diagnoses, to be introduced presently, pertaining to the putative blow-up give results that are virtually identical with those that obtain in the absence of dissipation, though the time t^* of blow-up is retarded by the dissipation. The value of δ_c depends upon the initial data of course. The computations show that for a slightly perturbed solitary wave of amplitude A, the critical value of δ_c has the form $\delta_c = \varepsilon A^p c_p$ where c_p is a constant depending only upon p. It is especially interesting to recall that the theoretical analysis of Section 2

showed unequivocally that for $p \geq 4$, there is a constant C_p such that if $\delta > \varepsilon A^p C_p$, then the solution emanating from initial data u_0 of amplitude A exists globally in time and decays to the mean of u_0 exponentially. This sharp agreement between analytically and numerically deduced information regarding a supposed scaling law for δ_c lends credence to its existence. Analogous numerical experiments for the zero$^{\text{th}}$-order dissipative problem (2.14) confirm the validity of a scaling law of the form (2.23) for σ_c.

With this background discussion and preview of some of the more important conclusions in hand, attention is now directed to a detailed description of the outcome of our numerical experiments. Reported first are computations for the initial- and periodic-boundary-value problem (1.3) with $p = 5, 6$ and 7. The borderline case $p = 4$ had already proved to be more difficult to understand when $\delta = 0$, and so it was not included in the present study. We first consider, as in the previous study, initial data which is a simple amplitude perturbation of a solitary-wave, to wit

$$u_0(x) = \lambda A \operatorname{sech}^{2/p}(K(x - \tfrac{1}{2})) \tag{4.3}$$

with K as in (2.12b) and with the perturbation parameter $\lambda > 1$ typically taken to be 1.01.

Consider the case with $A = 2.0$, $\lambda = 1.01$, $p = 5$ and $\varepsilon = 5 \times 10^{-4}$ which was studied with $\delta = 0$ in Bona *et al.* (1994). As seen clearly in Figure 6 of the last-quoted reference, the solitary wave rapidly lost it shape and its peak became unbounded, whilst exhibiting self-similar behavior. Let $M(t)$ be some norm of the solution emanating from (4.3), say, that becomes infinite in finite time. Its rate of blow-up is ρ where $M(t) \sim (t^* - t)^{-\rho}$ as $t \to t^*$, where t_* is as before, the blow-up time. The rate ρ is approximately equal to

$$\rho = \frac{-\log[M(\tau_1)/M(\tau_2)]}{\log[(\tau^* - \tau_1)/(\tau^* - \tau_2)]},$$

where τ_1, τ_2 are two distinct instances of $t < t^*$, but near t^*, where $M(t)$ is known.

The blow-up rates were computed for the approximate solution for the L_q-norms with $q = p-1,\ p,\ p+1,\ p+2,\ \infty$ and for the L_2- and L_∞-norms of its spatial derivative (denoted

$L_{2,D}$ and $L_{\infty,D}$, respectively). Naturally, the blow-up rates will not usually settle down to their asymptotic values until t is quite close to t^*. In Table 1 below are reproduced the numerically computed blow-up rates corresponding to the approximate solution emanating from the just-mentioned perturbed solitary wave at the times τ_i at which the computer code calls for the i^{th} spatial refinement. For details, the reader may consult Section 5 of Bona *et al.* (1994).

i	L_{p-1}	L_p	L_{p+1}	L_{p+2}	L_∞	$L_{2,D}$	$L_{\infty,D}$
5	.5029(-1)	.6683(-1)	.7795(-1)	.8590(-1)	.1336	.3008	.4657
10	.5047(-1)	.6729(-1)	.7853(-1)	.8657(-1)	.1348	.3028	.4731
15	.4983(-1)	.6647(-1)	.7759(-1)	.8554(-1)	.1334	.2992	.4618
20	.4989(-1)	.6658(-1)	.7773(-1)	.8572(-1)	.1338	.2999	.4690
25	.5044(-1)	.6728(-1)	.7851(-1)	.8654(-1)	.1347	.3029	.4747
30	.4974(-1)	.6633(-1)	.7741(-1)	.8534(-1)	.1329	.2985	.4685
35	.5001(-1)	.6672(-1)	.7786(-1)	.8583(-1)	.1336	.3004	.4654

Table 1

Blow-up rates. Perturbed Solitary wave, $p = 5$, $\varepsilon = 5 \times 10^{-4}$, $\delta = 0$,
$\tau_f = .22549 \times 10^{-1}$, $f = 42$, $x^* = .61333$, $U_{\max} = 224,766$,
$k_{\min} = .23 \times 10^{-40}$, $\Delta\tau_f = .16 \times 10^{-38}$.

The tolerance levels used to trigger the spatial and temporal refinements in the result represented in Table 1 were chosen on the basis of extensive computational experience. Simulations to be reported presently of the dissipative case utilized the same values of these parameters. In the legend of Table 1 are recorded the final time τ_f that is achieved after f spatial refinements, the approximate point $x^* \in [0,1]$ of blow-up and the amplitude $U_{\max}$ that the numerical approximation attained at $t = \tau_f$. The parameter $k_{\min}$ is the smallest time step arising in the computations and $\Delta\tau_f$ is the temporal increment the program made between the last two spatial refinements. Initially, the spatial meshlength was $h_0 = 1/192$ and the time step $k_0 = 10^{-3}$. It is useful to compare the blow-up rates in Table 1 to those that would obtain if the solution had the form depicted in (4.2). For

the reader's convenience, these hypothetical rates for the case $p = 5$ are displayed in Table 2. The agreement between corresponding values in Tables 1 and 2 lends credibility to the conjecture in (4.2). Graphs of the solution as a function of x for various values of t provided in Bona *et al.* (1994) also support the conclusion that the putative blow-up has a similarity form.

Norm	L_4	L_5	L_6	L_7	L_∞	$L_{2,D}$	$L_{\infty,D}$
Rate	.500(-1)	.667(-1)	.778(-1)	.857(-1)	.133	.300	.467

Table 2

Predicted blow-up rates according to (4.2) for $p = 5$.

What happens to the picture just outlined when dissipation is added? To approach this issue, we considered the approximation of a solution of (1.3) with all the parameters for the initial data as in the simulation just described except that δ was set to the positive value 2×10^{-4}. The parameters relating to the numerical scheme are also as above except that the initial time step k_0 was taken to be 1/1600 to minimize the numerical errors associated with the first stage of the integration.

The evolution in time of the approximate solution in the case of positive dissipation is depicted in the sequence of plots in Figure 1. The first four plots, which comprise Figure 1a, show the same response to the perturbation that was observed in the dissipationless case, namely the formation of a thin spike which proceeds to blow up at about the point $(x^*, t^*) = (.65812, .038624)$. In the graphs displayed in Figure 1a, the solution appears to blow up at $x_0 = 1/2$, but this is due to the occasional translations of the peak back to $x = 1/2$ to keep the maximum value of the solution located in the interval with the finest grid. This strategy allowed us to refine the spatial grid in a static way rather than moving the grid to follow the peak. (Actually, our simulations suggest that the center $X(t)$ of the peak at time t behaves according to the law $X(t) \sim x^* + C(t^* - t)^{1/3}$ as t approaches t^*, where C is some negative constant depending on δ, ε, p and u_0.) The second set of four

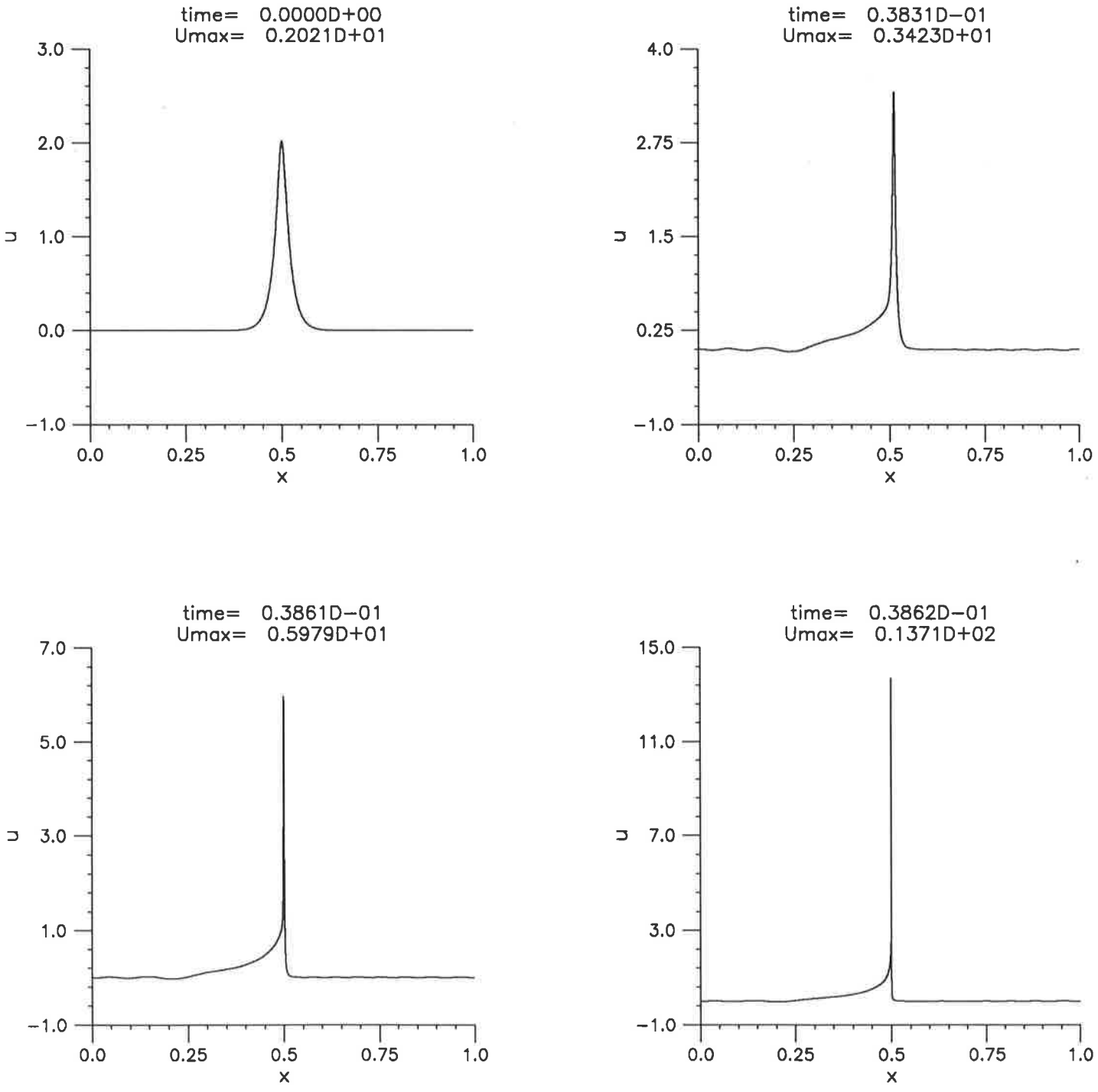

Figure 1a

Blow-up in the presence of small dissipation.

Perturbed solitary wave, $p = 5,\ A = 2,\ \lambda = 1.01,\ \varepsilon = 5 \times 10^{-4},\ \delta = 2 \times 10^{-4}$.

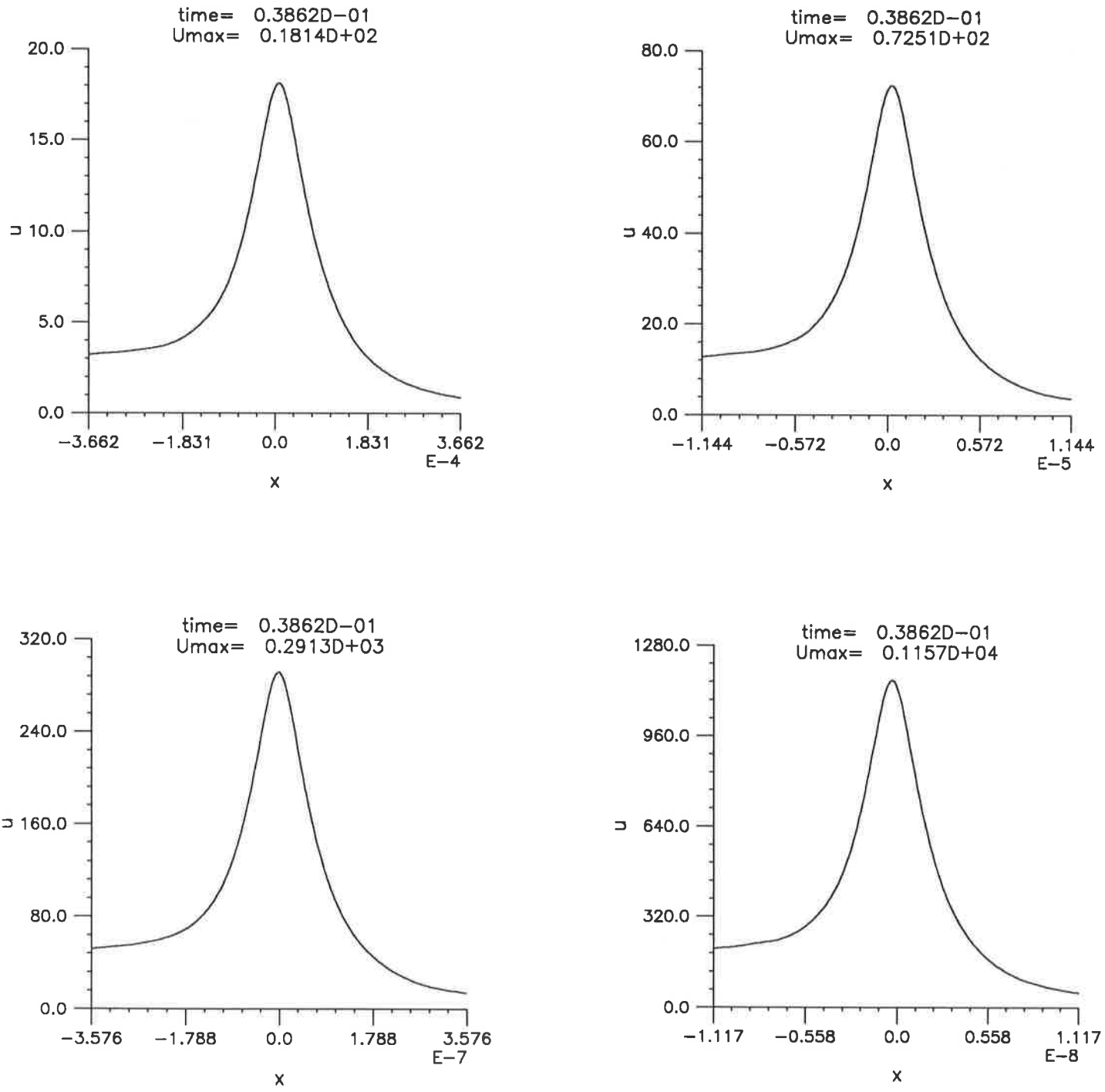

Figure 1b
Self-similarity of the blow-up. Data taken from the run of Figure 1a.

graphs in Figure 1b show, on a suitably rescaled set of x-t axes, a detailed view of the peak as it blows up. In these graphs the peak has been relocated to about $x = 0$ and the depiction is only that portion of the solution in the interval corresponding to the finest spatial grid (e.g. $[-6.81 \times 10^{-13},\ 6.81 \times 10^{-13}]$ in the fourth plot). These plots make plausible the presumption that there is a similarity structure through which the blow-up proceeds. Having determined that the solution corresponding to $\delta = 2 \times 10^{-4}$ and the previously mentioned perturbed solitary-wave initial data appears to form a singularity at a finite time t^*, it seemed appropriate to compute its blow-up rates near t^*. These are shown in Table 3, whose legend provides the precise values of all the parameters pertaining to this simulation. As in Table 1, there appears to be well-defined asymptotic blow-up rates associated with this solution, and, moreover, these blow-up rates are sensibly the same as those in Tables 1 and 2. Similar agreement in blow-up rates was observed in the analogous numerical experiments with perturbed solitary waves for $p = 6$ and 7. We also performed a set of experiments with initial data

$$u_0(x) = A\, e^{-100(x-\frac{1}{2})^2}, \tag{4.4}$$

which is a Gaussian profile not specifically tied to a travelling-wave solution of (1.1a). When an approximate solution was developed using our scheme and $A = 1$, $p = 5$, $\varepsilon = 2 \times 10^{-4}$ and $\delta = 10^{-4}$, it was found that the solution apparently blew up in finite time, at about the point $(x^*, t^*) = (.72886,\ .37376)$ where the approximate solution U had attained a value $U_{\max} = 17,148$. The form of the blow-up was much like that observed in the non-dissipative case (see §5 of Bona *et al.* 1994). In addition, the blow-up rates of the various norms of the solution emanating from the u_0 in (4.4) all agree to at least two digits with those for the solitary wave shown in Table 3. This lends further support to a scenario that is described as follows. The Gaussian initial data quickly resolves into a solution dominated by pulses that resemble solitary waves. The largest of these then becomes unstable and proceeds to form a singularity in finite time through the same route as seen already for the perturbed solitary wave in Figure 1.

i	L_{p-1}	L_p	L_{p+1}	L_{p+2}	L_∞	$L_{2,D}$	$L_{\infty,D}$
5	.5049(-1)	.6700(-1)	.7814(-1)	.8612(-1)	.1341	.3009	.4639
10	.4995(-1)	.6655(-1)	.7763(-1)	.8555(-1)	.1331	.2994	.4594
15	.5000(-1)	.6670(-1)	.7787(-1)	.8586(-1)	.1339	.3004	.4660
20	.4987(-1)	.6645(-1)	.7747(-1)	.8533(-1)	.1325	.2988	.4598
25	.5012(-1)	.6688(-1)	.7808(-1)	.8609(-1)	.1343	.3012	.4683
30	.5012(-1)	.6681(-1)	.7793(-1)	.8587(-1)	.1334	.3006	.4720
35	.5007(-1)	.6675(-1)	.7786(-1)	.8579(-1)	.1333	.3003	.4665

Table 3

Blow-up rates. Perturbed solitary wave initial data, $p = 5$, $\varepsilon = 5 \times 10^{-4}$, $\delta = 2 \times 10^{-4}$
$\tau_f = .38624 \times 10^{-1}$, $f = 39$, $x^* = .65812$, $U_{\max} = 98,050$, $k_{\min} = .60 \times 10^{-38}$,
$\Delta\tau_f = .77 \times 10^{-36}$.

It appears that the major effect of a small amount of dissipation added to the nonlinear, dispersive equation (1.1) is just to delay the blow-up. This is seen by comparing the approximate blow-up times τ_f in Tables 1 and 3. Since the peak propagates in the direction of increasing values of x, the blow-up point x^* is consequently translated to the right as well.

This paradigm changes as the level of dissipation increases. For example, repeating the numerical experiment corresponding to Figure 1, except with δ increased to 10^{-3}, the approximate solution was soon observed to develop dispersive oscillations followed by a steady decrease in the maximum amplitude (see Figure 2). By the time t had the value .09974, the largest excursion of the approximate solution was only about 1.03. A more detailed view of the temporal decay of this solution will be provided in the next subsection.

This pair of experiments pointed to the following possibility: For fixed initial data u_0 that leads to the formation of a singularity in finite time when $\delta = 0$, there is a critical value δ_c of δ such that solutions emanating from u_0 will form a singularity in finite time if $\delta < \delta_c$, and will exist globally in time if $\delta > \delta_c$.

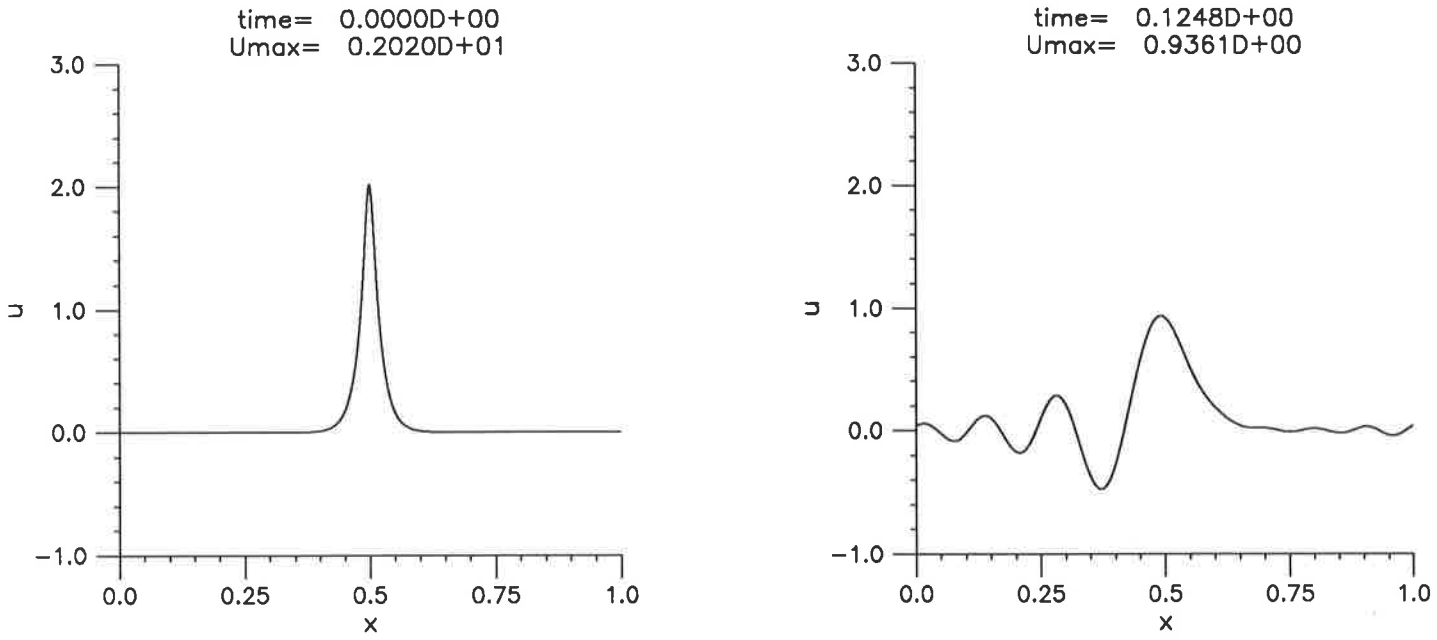

Figure 2

Oscillations and decay in the presence of larger dissipation.

Perturbed solitary wave, $p = 5,\ A = 2,\ \lambda = 1.01,\ \varepsilon = 5 \times 10^{-4},\ \delta = 10^{-3}$.

This hypothesis was copiously tested by several sequences of numerical experiments with perturbed solitary waves of the form (4.3) as initial data. Some of these results were presented in detail in Section 4 of Bona *et al.* (1992). On the basis of such experiments, a conjecture was stated in the just cited reference to the effect that there is a critical value c_p, depending only on p, of the parameter $\Delta = \delta^2\varepsilon/A^p$, such that if $\Delta < c_p$ the solution blows up at a point in finite time, while if $\Delta > c_p$, the solution exists for all t. The second part of this conjecture has now been proved (cf. Theorem 2.1 and subsequent remarks in Section 2; the constant C_p in (2.13) can be traced through the proof and, not surprisingly, turns out to be much larger than the experimentally observed value c_p.)

For a perturbed solitary-wave initial datum of the type (4.3) and a given set of parameters A, ε, p and λ (as mentioned before, we always took $\lambda = 1.01$ and experimented with $p = 5, 6$ and 7), we recorded two nearby values δ_c^- and δ_c^+ of the dissipation parameter, selected so that there was definite blow-up if $\delta \leq \delta_c^-$ and definite global existence and decay if $\delta \geq \delta_c^+$. As an example, we show the outcome of one such experiment corresponding to $p = 5,\ A = 2,\ \lambda = 1.01$, giving δ_c^- and δ_c^+ for various values of ε:

ε	δ_c^-	δ_c^+
.10(−3)	.10(−3)	.11(−3)
.25(−3)	.16(−3)	.17(−3)
.50(−3)	.230(−3)	.235(−3)
.80(−3)	.28(−3)	.30(−3)

The transition between 'definite' decay and 'definite' blow-up was quite sharp. This enabled us to define with some confidence a computationally determined version of the critical value δ_c to be the average of the sharpest achieved values δ_c^- and δ_c^+ after making the interval (δ_c^-, δ_c^+) as narrow as was computationally convenient.

In Table 4 we show, for $p = 5, 6$ and 7 and for various values of the amplitude A, the value of the parameter δ_c^2/ε. (This was computationally checked to be independent of ε for fixed A, p and λ; the particular data of Table 4 correspond to $\varepsilon = 5 \times 10^{-4}$). We also record the numbers $c_p = \delta_c^2/\varepsilon A^p$. The data clearly suggest that c_p is independent of A

and seems to be an increasing function of p, equal to about $.34 \times 10^{-5}$, 1.22×10^{-5}, and 2.42×10^{-5} for $p = 5, 6$ and 7, respectively.

A	$p = 5$		$p = 6$		$p = 7$	
	δ_c^2/ε	c_p	δ_c^2/ε	c_p	δ_c^2/ε	c_p
1.5	.026(-3)	.3483(-5)	.140(-3)	1.2330(-5)	.414(-3)	2.4233(-5)
2	.108(-3)	.3379(-5)	.781(-3)	1.2207(-5)	3.100(-3)	2.4219(-5)
2.5	.328(-3)	.3359(-5)	2.952(-3)	1.2093(-5)	1.485(-2)	2.4332(-5)
3	.832(-3)	.3424(-5)	8.862(-3)	1.2156(-5)	5.315(-2)	2.4302(-5)

Table 4
Critical values δ_c^2/ε and $c_p = \delta_c^2/\varepsilon A^p$
for blow-up of perturbed solitary wave initial value (4.3), $\lambda = 1.01$.

As discussed already, other classes of initial conditions resolve themselves into solitary waves plus a dispersive tail, even in the presence of dissipation. One would expect that if the largest solitary wave that emerges has amplitude A, then for δ large enough to guarantee the decay of this solitary wave, there should exist a global solution evolving from the given initial condition. On the other hand, if δ is such that the corresponding Δ is below its critical value, then it is expected that the solution will blow up in finite time.

We close this subsection with a brief computational study of the effect of the zero$^{\text{th}}$ order dissipation term σu on the behavior of solutions of the initial value problem (2.14) evolving from perturbed solitary-wave initial data of the form (4.3). As remarked in Section 2, if $\Sigma = (\sigma^2\varepsilon)^{1/3}/A^p$ is sufficiently large, a global solution exists, in fact decaying to zero in L_2 exponentially as $t \to \infty$. The numerical experiments conform to this fact and indicate that there exists a constant c_p', depending only on p, such that if $\Sigma < c_p'$ the solution blows up in finite time, whereas if $\Sigma > c_p'$ it will exist globally. In the event of blow-up, the blow-up rates were almost identical to the ones observed in the case of the (undamped) problem (1.1), suggesting that a similarity structure of the type (4.2) is formed again. Thus, the self-similar profile given by (4.2) proves to be quite stable under both types of dissipation

considered here. It should be noted that (2.14) seems to be a harder problem to integrate numerically up to blow-up as compared with (1.3), the reason probably being that as the blow-up is delayed by dissipation, small numerical oscillations may pollute somewhat the solution as it blows up. Such oscillations are likely to be damped more effectively by the second-order term $-\delta u_{xx}$.

Table 5 shows the results of a series of typical numerical experiments for $p = 5$ and various values of A, σ and ε. (We took $\lambda = 1.01$ as usual.) For a given value of A and σ, we varied ε and recorded a pair of nearby values ε_+ and ε_- chosen so that the interval $[\varepsilon_-, \varepsilon_+]$ was narrow, with definite blow-up as the outcome if $\varepsilon = \varepsilon_-$ and with definite global existence and decay if $\varepsilon = \varepsilon_+$. For the blow-up value, we also record $U_{\max}$ the maximum amplitude reached at the end of the computation, as well as τ_f, the approximate blow-up time. The critical value is indeed seen to be a constant, equal to about 1.8×10^{-3} independently of A, σ and ε.

A	σ	ε	Result	$U_{\max}$	τ_f	c'_p
1.7	.4	.11(-3)	decay			
		.10(-3)	blow-up	2071	.0776	1.804(-3)
1.8	.3	.44(-3)	decay			
		.43(-3)	blow-up	451	.1188	1.797(-3)
1.8	.4	.25(-3)	decay			
		.24(-3)	blow-up	2430	.0844	1.798(-3)
1.8	.5	.16(-3)	decay			
		.15(-3)	blow-up	1951	.0607	1.791(-3)
1.9	.4	.56(-3)	decay			
		.55(-3)	blow-up	107	.1030	1.802(-3)

Table 5

Blow-up and decay of (2.14). Perturbed solitary wave initial data, $\lambda = 1.01$, $p = 5$.

The computed critical value of $\Sigma = (\sigma^2 \varepsilon_c)^{1/3}/A^p$ is given in the last column of the Table. (The value ε_c was taken as the average of the two recorded values ε_+ and ε_- of ε.)

4B. DECAY OF SOLUTIONS

In this section attention is restricted to the periodic initial-value problem (1.3) for the generalized Korteweg-de Vries-Burgers equation in which the spatial period of the initial data and the corresponding solution is normalized to be $L = 1$. The dissipation parameter δ is taken large enough that the problem has a global solution. In this case, it follows from Corollary 2.3, that the solution of (1.3) decays in L^2 exponentially fast, indeed, satisfying

$$|u(\cdot,t) - \overline{u}_0|_2 \leq e^{-(2\pi)^2\delta t}|u_0 - \overline{u}_0|_2, \tag{4.5}$$

where $\overline{u}_0 = \int_0^1 u_0(x)dx$. In addition, if u_0 belongs to $H^s(0,1)$, and satisfies the smallness condition (2.9) relative to δ, then all seminorms $|\partial_x^j u|_2$, $1 \leq j \leq s$, decay exponentially to zero as t grows. (In Corollary 2.3 the proof given yields that $|u_x(\cdot,t)|_2$ decays with a rate of $O(e^{-(2\pi)^2\delta' t})$ for some constant δ' with $0 < \delta' < \delta$.)

As may already be gleaned from the example presented in the previous subsection (cf. Figure 2), the solution evolving from, say, a solitary-wave initial profile, breaks up, develops an oscillatory tail that travels around due to periodicity and interacts with the bulk of the wave, thereby producing an irregular pattern of oscillations. As t grows, the various modes of the solution decay, with the highest ones vanishing first. Eventually, the solution settles down to a sinusoidal profile which decays to the constant $\overline{u}_0$ while travelling with a speed determined by $\overline{u}_0$ and the dispersive term in (1.3). Thus, for very large values of t, the solution is essentially governed by the linearized equation corresponding to (1.2).

In the first part of this section we shall study, by means of numerical experiments, the details of the just outlined behavior of the long-time decay of solutions. In the second part we shall present numerical examples illustrating the short-time oscillatory break-up of solutions and provide a brief commentary on this phenomenon.

Biler (1984), using techniques of Foias and Saut (1984), has proved sharp decay estimates as $t \to \infty$ for the solutions of a class of nonlinear dispersive equations with dissipation, posed on an interval with periodic boundary conditions. His theory covers the initial-

and periodic-boundary-value problem (1.3) for $\overline{u}_0 = 0$ and $p < 2$, and shows, essentially, that $\lim_{t\to\infty} \frac{\log|u(t)|_2}{t} = \lim_{t\to\infty} \frac{\log|u_x(t)|_2}{t} = -\delta\Lambda$ where Λ depends on u_0 and is one of the eigenvalues $(2\pi n)^2$, $n = 1, 2\ldots$, of the operator $-\frac{d^2}{dx^2}$ on $[0,1]$ (i.e. of the differential operator in the dissipative term), with periodic boundary conditions at the endpoints. Hence, both $|u|_2$ and $|u_x|_2$ are $O(e^{-\delta\Lambda t})$ as $t \to \infty$. Here, for two types of initial conditions u_0, and for $p = 5$ and 6, we shall present computational evidence which, among other things, suggests that in various norms the solution of (1.3) decays to $\overline{u}_0$ in such a way that it is $O(e^{-(2\pi)^2\delta t})$ as $t \to +\infty$. In particular, the decay rate in (4.5) appears to be sharp.

In a first experiment, we took $p = 5$, $\varepsilon = 0.5 \times 10^{-3}$, $\delta = 0.2 \times 10^{-3}$, and, as initial value, the perturbed solitary wave of the form (4.3) with $A = 1.5$, $\lambda = 1.01$, and mass $\overline{u}_0 = .141258$. For all norms or seminorms $M(\cdot)$ (see below) considered, it was observed that the decay was indeed exponential We then determined for each quantity M the constants B and μ such that

$$M(u(t) - \overline{u}_0) \simeq Be^{-\mu t}, \quad \text{as} \quad t \to \infty. \tag{4.8}$$

This was accomplished by computing $M_i = M(u(t_i) - \overline{u}_0)$ at times $t_i = t_0 + i\Delta t$, $i = 1, 2, \ldots$, where $\Delta t = 2$, and determining for each i the values

$$\mu_i = \frac{-1}{\Delta t} \log\left(\frac{M_i}{M_{i-1}}\right).$$

and

$$B_i = M_i \exp\,(\mu_i t_i)$$

The results are shown in Table 6 for t up to 500. The quantities $M(v)$ are the norms $|v|_q, q = 2, p, \infty$, and also, the seminorms $|v_x|_2$ and $|v_x|_\infty$. For each M and different values of t_i, the corresponding computed values of μ_i and B_i are recorded in Table 6a and Table 6b, respectively. We also show the rates and constants for the $|v|_q$ norms for $q = p - 1$, $p + 1$ and $p + 2$ only at the final instance $t = 500$ since their evolution with increasing t closely resembles that of the entries of the L^p column.

t	L_2	L_p	L_∞	$L_{2,D}$	$L_{\infty,D}$
20	.15061(-1)	.49132(-1)	.10203	.37086(-1)	.18847
40	.10434(-1)	.14300(-1)	.15728(-1)	.16468(-1)	.48906(-1)
60	.89678(-2)	.53166(-2)	-.33487(-1)	.99156(-2)	.36859(-1)
80	.83190(-2)	.10563(-1)	.41326(-1)	.10284(-1)	-.18133(-1)
100	.80498(-2)	.86300(-2)	.19954(-1)	.84097(-2)	-.62585(-2)
200	.78970(-2)	.78983(-2)	.49293(-2)	.79085(-2)	.14790(-1)
300	.78957(-2)	.78961(-2)	.83062(-2)	.78961(-2)	.76502(-2)
400	.78957(-2)	.78957(-2)	.79115(-2)	.78957(-2)	.78744(-2)
500	.78957(-2)	.78957(-2)	.78934(-2)	.78957(-2)	.79025(-2)

t	L_{p-1}	L_{p+1}	L_{p+2}
500	.78957(-2)	.78957(-2)	.78957(-2)

Table 6a

Decay parameters μ. Perturbed solitary-wave initial profile, $p = 5, \delta = 0.2 \times 10^{-3}, \varepsilon = 0.5 \times 10^{-3}$.

t	L_2	L_p	L_∞	$L_{2,D}$	$L_{\infty,D}$
20	.28507	.70903	2.88439	3.78547	125.11658
40	.25131	.34881	.52391	2.29930	16.33909
60	.23425	.22288	.31065(-1)	1.65868	14.17259
80	.22425	.30862	4.66287	1.68911	.29991
100	.21903	.26574	1.06674	1.44014	.52915
200	.21504	.24510	.16915	1.35432	7.59734
300	.21498	.24498	.34389	1.35089	1.77678
400	.21497	.24495	.30599	1.35072	1.89423
500	.21497	.24495	.30368	1.35072	1.91675

t	L_{p-1}	L_{p+1}	L_{p+2}
500	.23791	.25044	.25487

Table 6b

Decay parameters B. Perturbed solitary-wave initial profile, $p = 5, \delta = 0.2 \times 10^{-3}, \varepsilon = 0.5 \times 10^{-3}$.

We observe that after an initial transient stage, the $L_q, q = 2, p-1, p, p+1, p+2$ and $L_{2,D}$ rates μ and the associated B's stabilize to constant values. The L_∞ and $L_{\infty,D}$ values also stabilize after a larger time period has elapsed; this probably reflects rougher actual decay of these norms and the extra difficulty generally encountered in pointwise approximation. The eventual rate of decay that emerges from the $L_q, q \leq p+2$ and $L_{2,D}$ columns is clearly $\mu = .78957(-2)$. This is an accurate approximation of $(2\pi)^2\delta = .789568\ldots(-2)$ to five significant digits. The L_∞ and $L_{\infty,D}$ values have three, respectively two, correct digits. It seems safe to conclude then from this experiment that all norms of $u - \overline{u}_0$ decay exponentially in time with decay rate $\mu = (2\pi)^2\delta$ and constants B that depend on the particular norm measured.

In a subsequent experiment, the dissipation constant was doubled to $\delta = .4 \times 10^{-3}$ while keeping all other parameters the same. As a result of the larger value of δ, the decay is faster and the entries stabilized *grosso modo* by $t = 140$. The results are shown (at $t = 140$ only) in Table 7, and confirm the decay rate $\mu = (2\pi)^2\delta$; here the exact value is $(2\pi)^2\delta = .157914(-2)$. We also observe that for all norms the constants B have decreased almost uniformly by about one percent; hence these constants probably depend weakly on δ.

Norm	μ	B
L_2	.15791(-1)	.21269
L_{p-1}	.15792(-1)	.23540
L_p	.15792(-1)	.24237
L_{p+1}	.15792(-1)	.24781
L_{p+2}	.15792(-1)	.25219
L_∞	.15549(-1)	.29101
$L_{2,D}$	.15792(-1)	1.33652
$L_{\infty,D}$	.16900(-1)	2.20768

Table 7
Decay parameters μ and B at $t = 140$.
Perturbed solitary-wave initial profile, $p = 5$, $\delta = 0.4 \times 10^{-3}$, $\varepsilon = 0.5 \times 10^{-3}$.

It should be mentioned that the decay rate $(2\pi)^2\delta$ was confirmed for all the norms and seminorms considered in analogous numerical experiments with a pertrubed solitary-wave initial profile in the case $p = 6$. Finally we experimented with a Gaussian initial profile of the form (4.4) (for which $\overline{u}_0 = .177245$), taking $p = 5$, $\varepsilon = .2 \times 10^{-3}$, $\delta = 10^{-3}$ in (1.3) and integrating up to $t = 80$ by which time the constants μ and B for each norm and seminorm under consideration (including both the L_∞ and $L_{\infty,D}$ entries) had stabilized. The results are shown in Table 8. The computational decay rate μ is again seen to be very close to the value $(2\pi)^2\delta = .394784(-1)$ hypothesized earlier.

Norm	μ	B
L_2	.39478(-1)	.21532
L_{p-1}	.39479(-1)	.23830
L_p	.39479(-1)	.24536
L_{p+1}	.39479(-1)	.25086
L_{p+2}	.39479(-1)	.25530
L_∞	.39496(-1)	.30514
$L_{2,D}$	.39478(-1)	1.35293
$L_{\infty,D}$	.39473(-1)	1.91312

Table 8
Decay parameters μ and B at $t = 80$.
Gaussian initial profile, $p = 5$, $\delta = 10^{-3}$, $\varepsilon = .2 \times 10^{-3}$.

A sample of the simulated temporal evolution of solutions corresponding to the solitary-wave initial condition that yielded the results of Table 6, and to the Gaussian initial condition from which Table 8 was produced, is shown in the sequence of plots of Figures 3 and 4, respectively. In both cases the solutions eventually settle down to profiles resembling sinusoidal waves travelling slowly to the left as they decay to their respective values of $\overline{u}_0$.

An inspection of the first few terms of the series solution of a linear problem associated to (1.2) proves quite illuminating. Defining $\omega(x,t) = u(x,t) - \overline{u}_0$, one expects that since

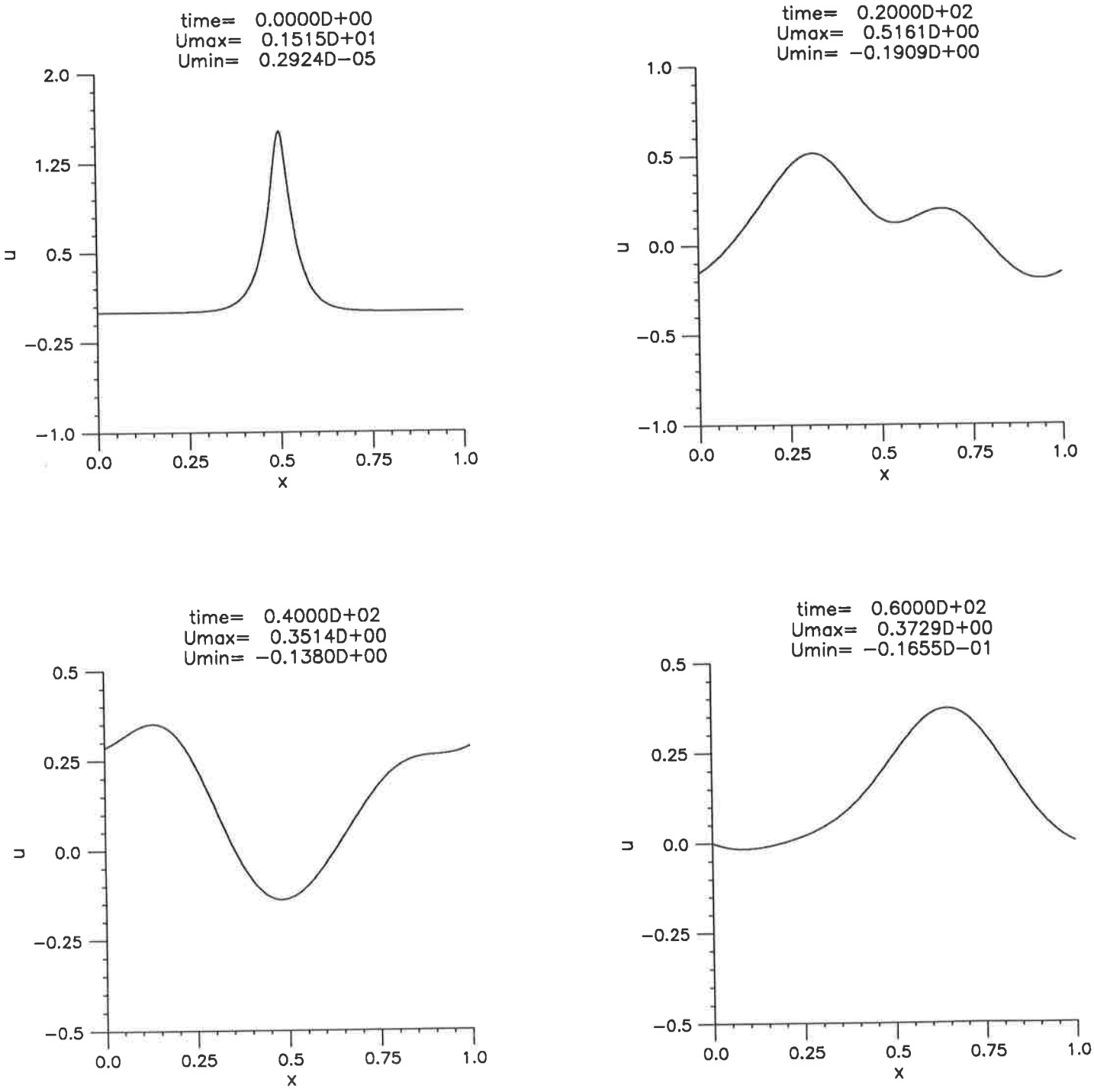

Figure 3a
Long-time decay of solitary-wave initial data. Parameters of Table 6.

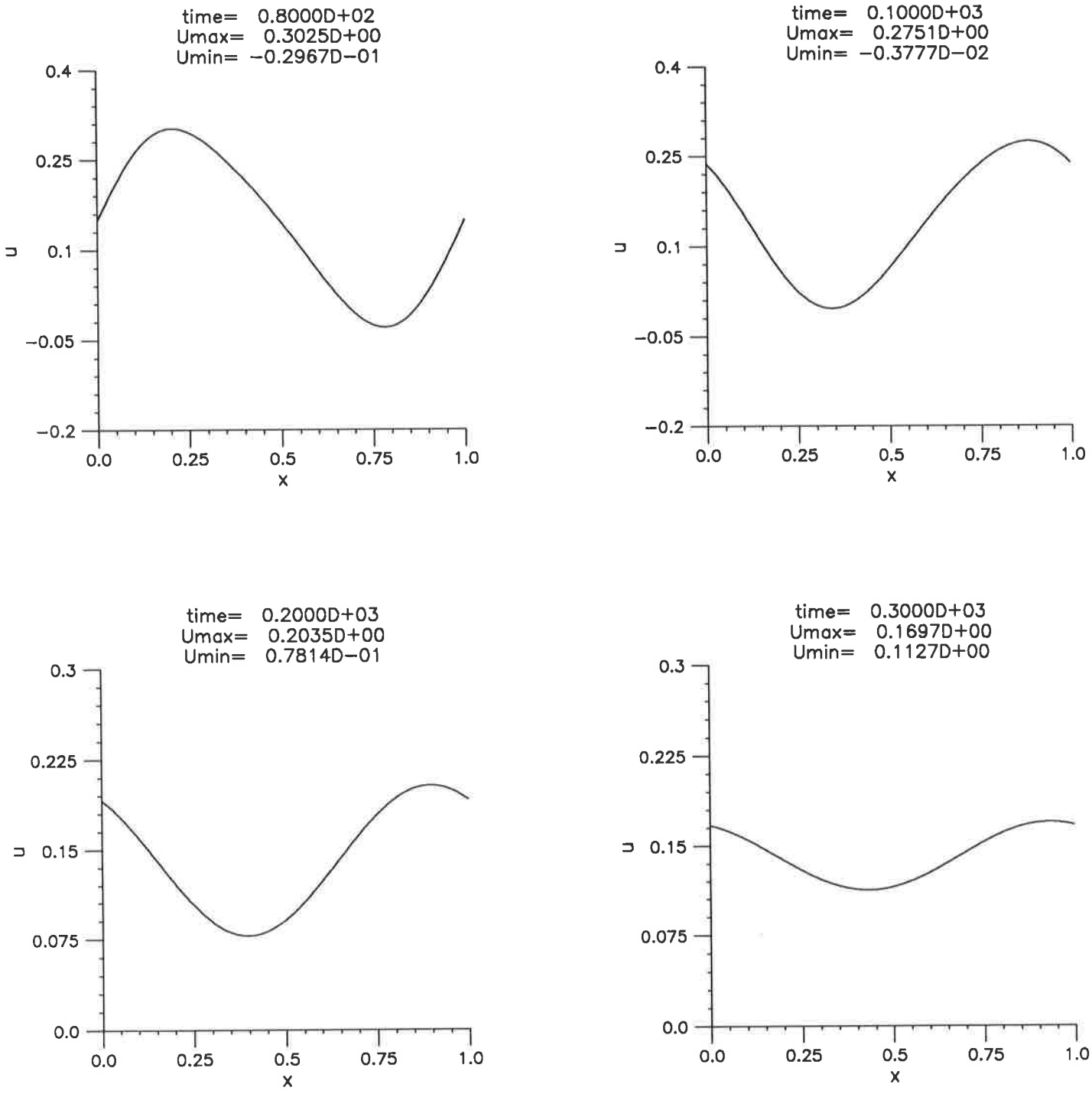

Figure 3b
Long-time decay of solitary-wave initial data, continued.

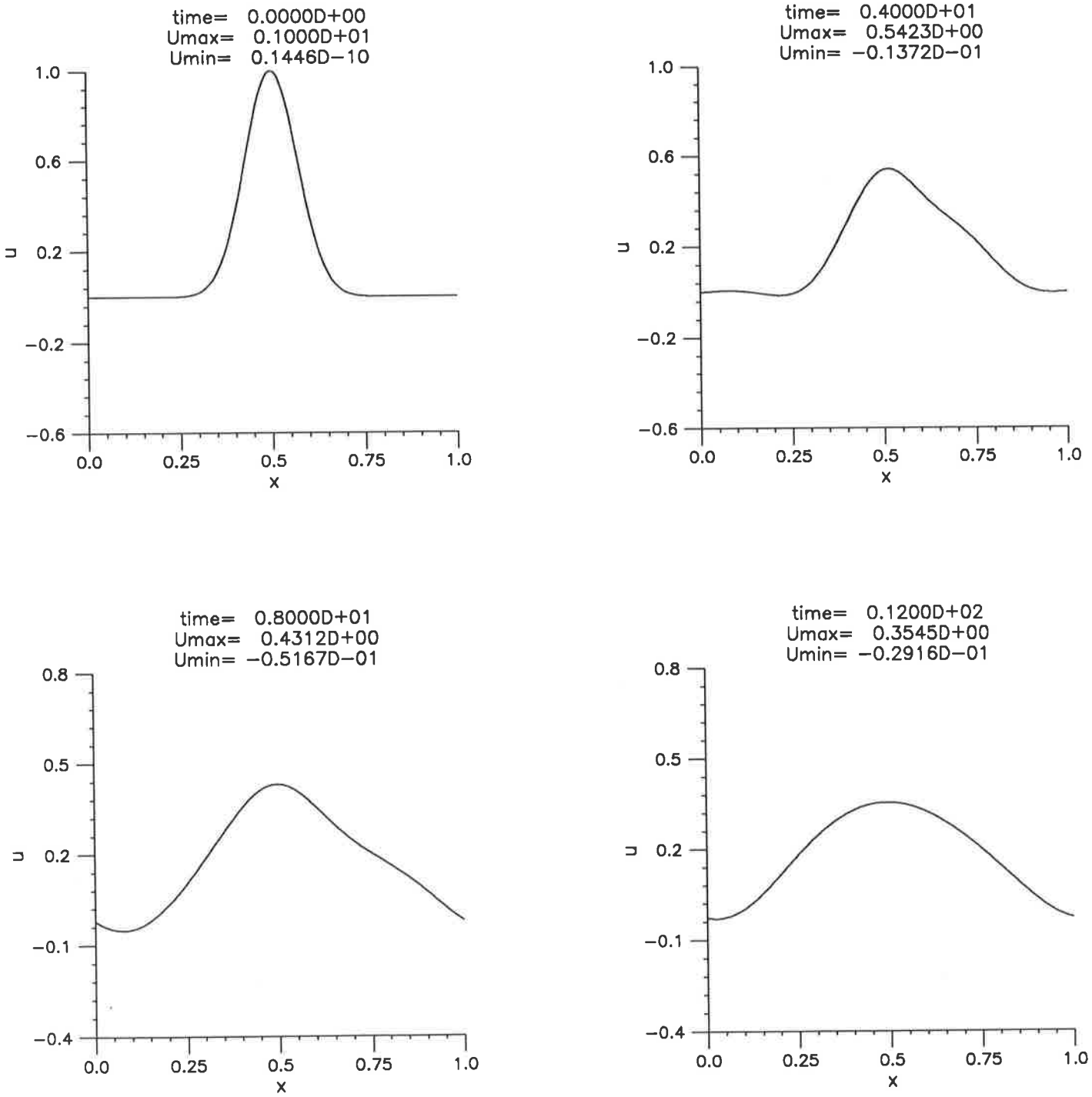

Figure 4a
Long-time decay of Gaussian initial data. Parameters of Table 8.

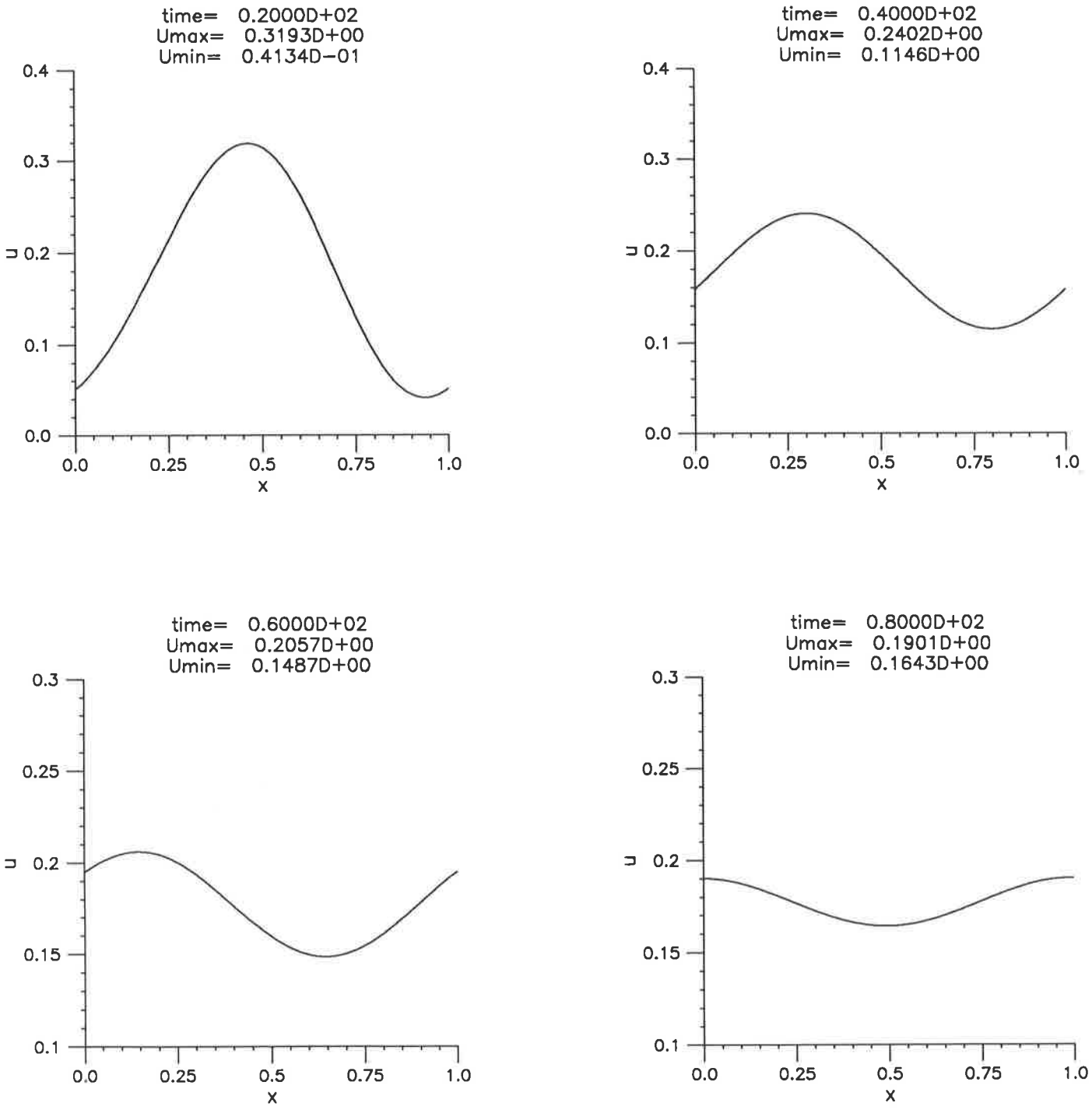

Figure 4b
Long-time decay of Gaussian initial data, continued.

ω tends to zero as t becomes large, for large t the function ω approximately satisfies the linearized dispersive-dissipative equation

$$\omega_t + \eta\omega_x - \delta\omega_{xx} + \varepsilon\omega_{xxx} = 0, \tag{4.7}$$

where $\eta = \overline{u}_0^p$. The solution of (4.7) posed with periodic boundary conditions on $[0,1]$ and with initial condition equal to the 1-periodic function $\omega_0(x) = u_0(x) - \overline{u}_0$ is given by the Fourier series

$$\omega(x,t) = \sum_{n\in\mathbb{Z}} a_n e^{-\delta(2\pi n)^2 t}\, e^{2\pi i n[x-(\eta-\varepsilon(2\pi n)^2)t]},$$

where $a_n = \int_0^1 \omega_0(x)e^{-2\pi i n x}dx$, $n \in \mathbb{Z}$, $a_0 = 0$. Keeping only the lowest frequency, exponentially decaying terms yields the approximation

$$\omega(x,t) \simeq \alpha e^{-(2\pi)^2\delta t}\cos\left\{2\pi[x-(\eta-(2\pi)^2\varepsilon)t]-\xi\right\}, \tag{4.8}$$

where the amplitude coefficient α and the phase shift ξ are constants depending only on the first Fourier components $\int_0^1 \omega_0(x)e^{\pm 2\pi i x}dx$ of ω_0. The relation (4.8) predicts the dominant exponential decay rate $O(e^{-(2\pi)^2\delta t})$ as $t \to \infty$ for solutions of the linear equation; as we have seen this was also observed in the numerical experiments with the nonlinear equation for $u(x,t) - \overline{u}_0$ for very large values of t. It also predicts that the decaying solution asymptotically resembles $\overline{u}_0$ plus a sinusoidal wave profile that, as it decays in amplitude, travels with a speed equal to $\eta - (2\pi)^2\varepsilon = (\overline{u}_0)^p - (2\pi)^2\varepsilon$. This is actually quite close to the value that can be obtained from the output of our numerical experiments. As an example, for the run corresponding to Table 6 and Figure 3, (4.8) predicts a speed equal to -0.01968, which is an excellent approximation to the numerical speed observed in the experiment and computed as follows. Let $X(t)$ denote the point in $[0,1]$ where $u(x,t)$ attains its maximum. Using $t_i = 2(i-2)$, $i \geq 3$ and measuring the speed of the travelling wave at time t_i by the ratio $v_i = (X(t_i) - X(t_{i-1}))/(t_i - t_{i-1})$ (where the variable X is viewed as an element of $\mathbb{R}/Z$ and distances computed accordingly) one obtains Table 9 showing the values of $X(t)$ and v at large values of t_i.

t_i	$X(t_i)$	v_i
200	.8975	-.1853(-1)
300	.9306	-.1971(-1)
400	.9629	-.1967(-1)
500	.9948	-.1962(-1)

Table 9
Long-time speed of the travelling wave, example of Table 6.

Similarly, for the run with a Gaussian initial profile whose evolution was described in Table 8 and Figure 4, (4.8) predicts a speed v equal to $-.00772$. The actual value of v at $t = 80$ was $-.00781$.

Of course the linearized equation provides qualitative information only for very large values of t, when the nonlinear term has ceased to be of any importance. For intermediate values of t, the solution may decay in a complicated way, with energy being exchanged between the lower and the higher modes; in fact, it can be the case that, initially, some of the lower modes will actually increase for a short time due to the nonlinearity. This history of nonlinear decay ought to be reflected, for example, in the constants B in (4.6), which cannot be predicted solely in terms of u_0 as in the linear case. In fact, the weak dependence of B on δ observed in Tables 6 and 7 is probably due to the nonlinearity in the problem. See Amick *et al.* 1989 for commentary on the role of nonlinearity in decaying solutions of (1.2) when the initial-value problem is posed on the entire real line.

Turning now to the short-time decay of solutions of (1.3) and to the formation of the oscillatory tail, we show in Figure 5 the short-time ($0 \leq t \leq 0.2$) evolution, in the case $p = 5$, of an initially unperturbed solitary wave of amplitude $A = 2$, when $\delta = \varepsilon = 0.5 \times 10^{-3}$. The oscillatory tail forms, travels around due to periodicity and starts interacting with the remnant of the main pulse which has not moved appreciably. If the amplitude of the solitary wave is increased, it is observed that the oscillations become more numerous,

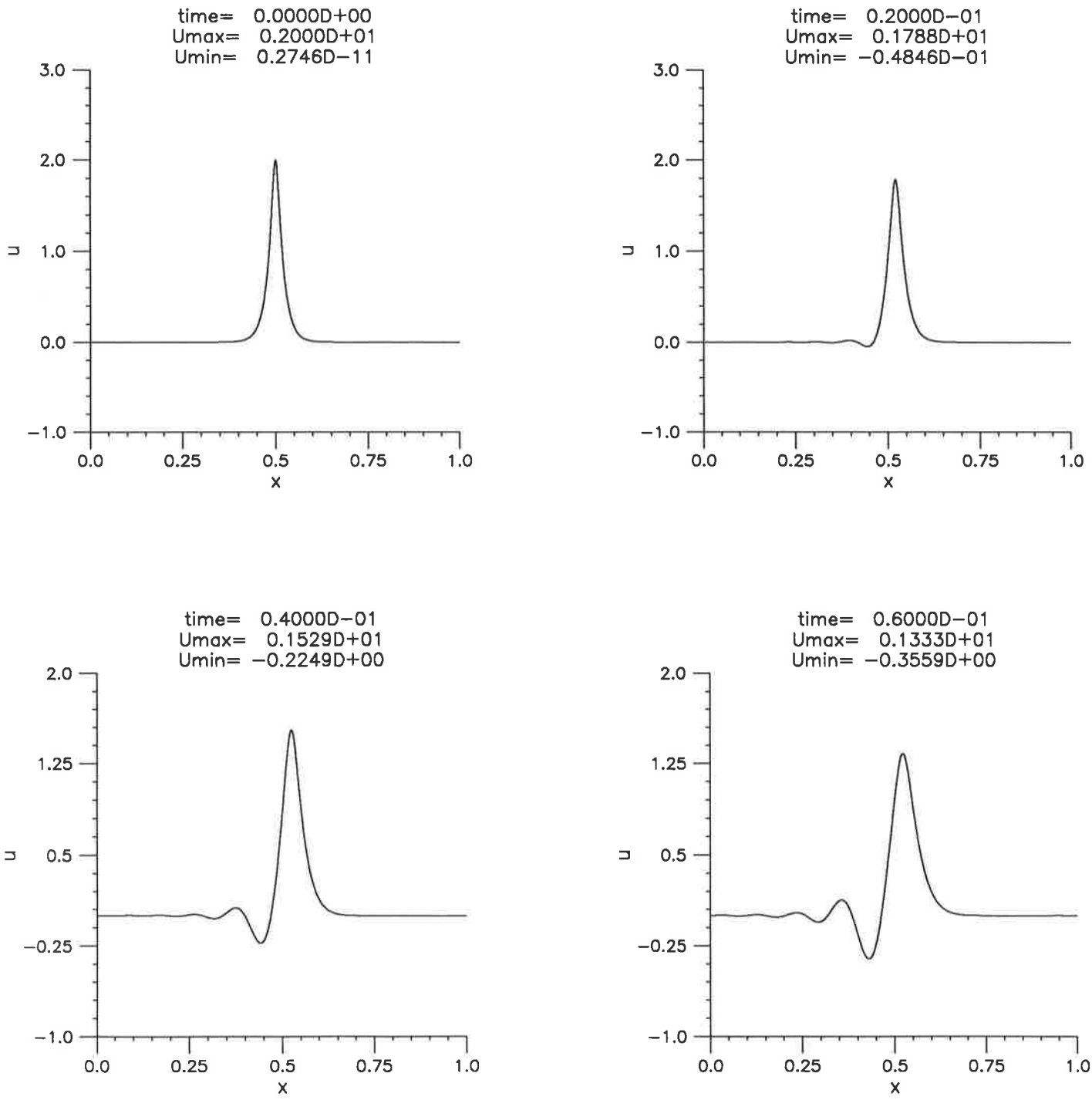

Figure 5a

Initial decay of solitary-wave initial data with $A = 2$, $\varepsilon = 0.5 \times 10^{-3}$, $\delta = 0.5 \times 10^{-3}$.

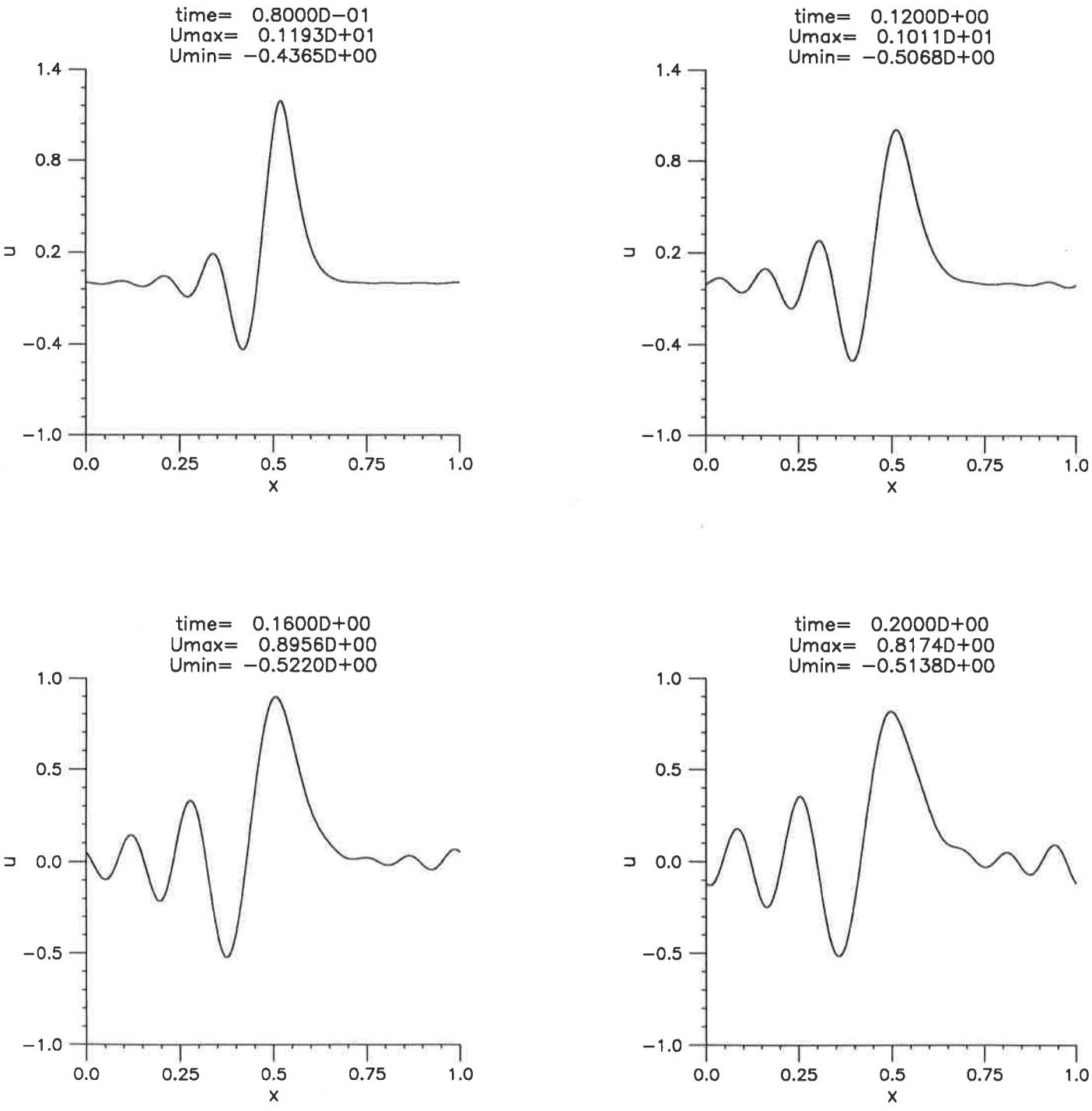

Figure 5b
Initial decay of solitary-wave initial data, continued.

better formed and travel faster. Finally, Figure 6 shows the interesting initial decay of the Gaussian $u_0(x) = e^{-100(x-1/2)^2}$, allowed to evolve under (1.3) with parameters $p = 5$, $\varepsilon = 0.2 \times 10^{-3}$ and $\delta = 0.6 \times 10^{-3}$. The initial profile attempts to resolve itself into solitary-wave pulses that actually grow in amplitude for a while. Had δ been smaller, the leading one would have proceeded to blow-up, as the numerical evidence presented in Section 4a and Bona *et al,* (1994) shows. But, here eventually, the dissipative term dominates and dictates the decay.

5. CONCLUSIONS

The overarching goal of the preceding discussion was to better understand the additional effect of dissipation on solutions of nonlinear, dispersive wave equations. The present study centered around dissipative perturbations of the generalized Korteweg-de Vries equation (1.1a), but it is expected that the information gleaned for this class of equations will provide useful guidance in other, related equations.

It is not surprising that even a small amount of dissipation will substantially alter much of the long-term behavior of solutions. For example, the solitary waves that often appear to play such a fundamental role in the long-term evolution of solutions of initial-value problems like (1.1) for L_2-initial data cease to exist in the face of dissipation. (However, steadily propagating bore-like solutions may well exist in dissipative cases – cf. Bona & Schonbek 1985 and Bona, Rajopadhye & Schonbek 1994.)

The principal focus here has been to comprehend the effect of dissipation on the putative singularity formation observed in (1.1) when $p \geq 4$. The conclusions that form as a result of the information obtained from our numerical experiments are compactly summarized as follows. For suitable s, say $s \geq 2$, let initial data $g \in H^s$ be given. Consider a dissipative perturbation of (1.1a) such as the GKdV-Burgers equation (1.3) or the model (2.14). Let $\nu \geq 0$ connote a parameter like δ in (1.3) or σ in (2.14) that specifies the strength of the perturbation relative to to that of the nonlinear and dispersive terms. Let

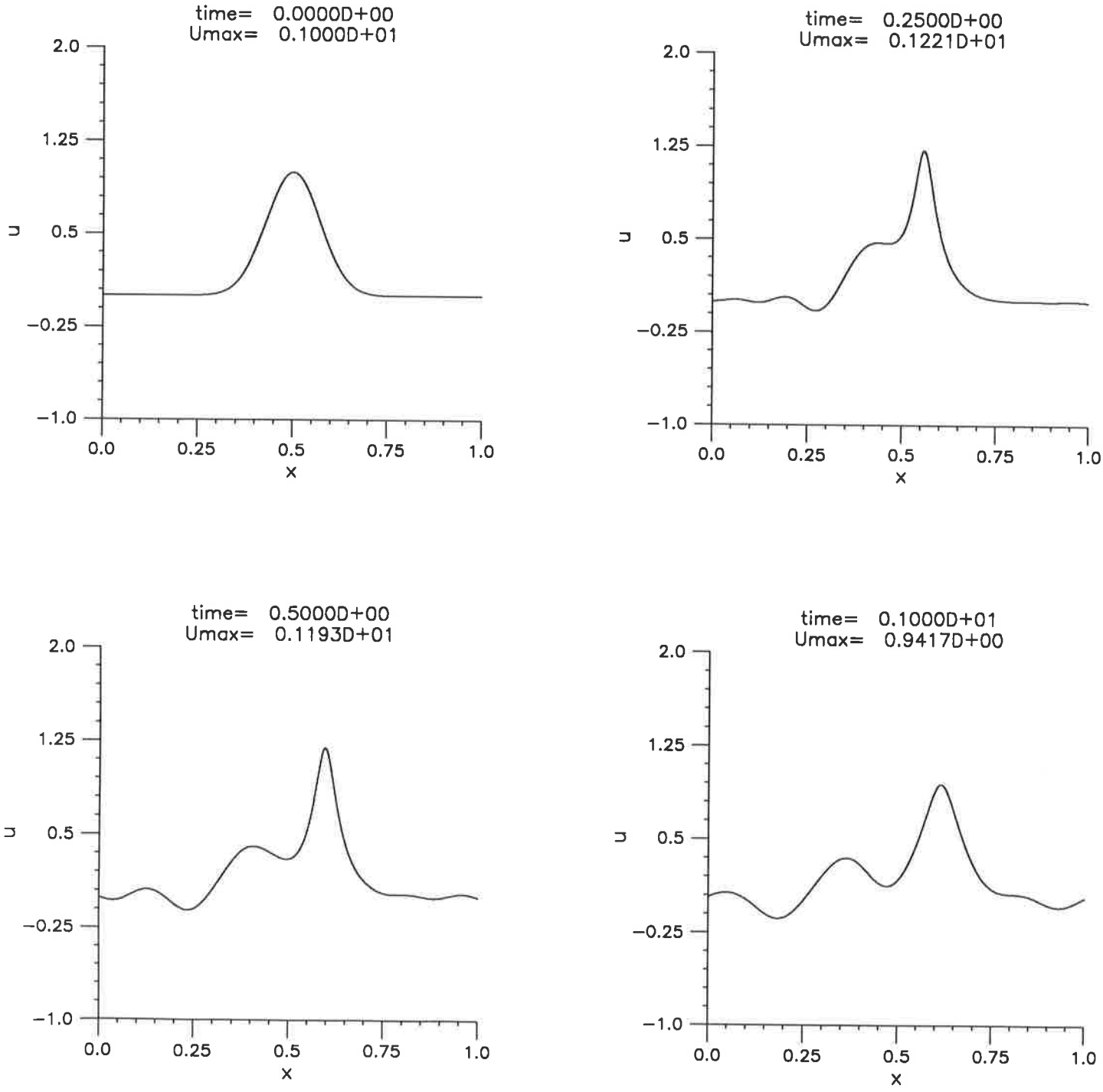

Figure 6
Initial decay of Gaussian initial data $p = 5$, $\varepsilon = 0.2 \times 10^{-3}$, $\delta = 0.6 \times 10^{-3}$.

T_ν denote the maximum existence time for the H^s-solution of the relevant initial-value problem with initial datum g and dissipative parameter ν. That is, for any T in $[0, T_\nu)$, there is a unique H^s-solution defined on $[0, T]$ and T_ν is maximal in this regard. The existence time T_ν is always positive on account of the local well-posedness of the initial-value problem, and either $T_\nu = +\infty$ or the L_∞-norm of the solution becomes unbounded as t approaches T_ν (see Kato 1983, Bona *et al.* 1988). Moreover, simple scaling arguments together with the continuous dependence results make plausible the conjecture that T_ν is an increasing function of ν. The outcome of the numerical experiments reported in Section 4 then indicate the following dichotomy: either

(i) $T_0 = +\infty$, in which case $T_\nu = +\infty$ for all $\nu > 0$,

or

(ii) $T_0 < +\infty$, in which case there exists a critical value ν_c with $0 < \nu_c < +\infty$ such that $T_\nu < +\infty$ for all $\nu < \nu_c$ and $T_\nu = +\infty$ for $\nu \geq \nu_c$.

In the second case, we expect T_ν to be a non-decreasing function of $\nu \in \mathbb{R}^+$ with values in the extended positive real numbers $\mathbb{R}^+ \cup \{+\infty\}$, and continuous except perhaps at ν_c where there may be a jump discontinuity.

If $T_0 < +\infty$, then our experiments also indicate that the structure through which singularity formation occurs varies only slightly with ν until ν_c is reached. However, the two different dissipative mechanisms considered showed a different dependence upon the parameter p.

It would be interesting and relevant to important modelling situations to broaden the range of dissipative mechanisms considered. A natural class of local dissipative terms that deserves consideration in conjunction with the GKdV equation is $(-1)^j \partial_x^{2j}$, $j = 2, 3, \ldots$. It is straightforward to determine that the initial-value problem for the GKdV equation with the term $\nu(-1)^k \partial_x^{2k} u$, $\nu > 0$ appended is globally well posed for arbitrary sized initial data if $p < 4k - 2$. It could be instructive to learn what happens if $\nu > 0$, $k \geq 2$ and $p > 4k - 2$. The case $k = 2$ may already be quite different from the cases $k = 0$ and $k = 1$

examined here because for $k \geq 2$ the critical value of the parameter p in the nonlinearity is determined solely by the dissipative term rather than the dispersive term. Non-local dissipative processes also arise as models in practically interesting situations. Broadening still further the range of inquiry might lead to the GKdV equation with dissipative perturbation $\nu M_\alpha u$, where $\hat{M_\alpha v}(\xi) = |\xi|^\alpha \hat{v}(\xi)$ is a homogeneous Fourier multiplier operator. The decay of solutions of the initial-value problem

$$u_t + u^p u_x + u_{xxx} + \nu M_\alpha u = 0,$$

$$u(x,0) = g(x)$$

has been studied when g is suitably small (see Dix 1992, Bona, Promislow & Wayne 1994, Bona & Demengel 1994). However, the situation that obtains for larger initial values has thus far resisted analysis, and careful numerical simulation would be welcome.

Acknowledgements

The authors gratefully acknowledge support and hospitality from the Institute of Applied and Computational Mathematics at the Research Center of Crete, FORTH, and the Mathematics Department at Penn State. The collaboration was materially aided by a joint travel grant from the National Science Foundation, USA, and the General Secretariat of Research & Technology, Greece. JLB and OAK also acknowledge general support from the National Science Foundation and the University of Tennessee Science Alliance.

References

Albert, J.P. & Bona, J.L. 1991 Comparisons between model equations for long waves. *J. Nonlinear Sci.* **1**, 345–374.

Albert, J.P., Bona, J.L. & Felland, F. 1988 A criterion for the formation of singularities for the generalized Korteweg-de Vries equation. *Mat. Aplic. e Comp.* **7**, 3–11.

Amick, C.J., Bona, J.L. & Schonbek, M.E. 1989 Decay of solutions of some nonlinear wave equations. *J. Diff'l. Eqns.* **81**, 1–49.

Baker, G., Dougalis, V.A. & Karakashian, O.A. 1983 Convergence of Galerkin approximations for the Korteweg-de Vries equation. *Math. Comp.* **40**, 419–433.

Benjamin, T.B. 1974 Lectures on nonlinear wave motion. In *Lectures in Applied Mathematics* **15**, pp. 3–47, (A. Newell, ed.) American Math. Soc.: Providence.

Benjamin, T.B., Bona, J.L. & Mahony, J.J. 1972 Model equations for long waves in nonlinear, dispersive media. *Philos. Trans. Royal Soc. London A* **272**, 47–78.

Biler, P. 1984 Large-time behaviour of periodic solutions to dissipative equations of Korteweg-de Vries-Burgers type. *Bull. Polish Acad. Sci. Math.* **32**, 401–405.

Bona, J.L. 1981 Convergence of periodic wave trains in the limit of large wavelength. *Appl. Sci. Res.* **37**, 21–30.

Bona, J.L. & Demengel, F. 1994 Non-local dissipation and the decay of nonlinear dispersive waves. To appear.

Bona, J.L., Dougalis, V.A. & Karakashian, O.A. 1986 Fully discrete Galerkin methods for the Korteweg-de Vries equation. *Comp. & Maths. with Applics.* **12A**, 859–884.

Bona, J.L., Dougalis, V.A., Karakashian, O.A. & McKinney, W.R. 1992 Computations of blow-up and decay for periodic solutions of the generalized Korteweg-de Vries equation. *Appl. Numerical Math.* **10**, 335–355.

Bona, J.L., Dougalis, V.A., Karakashian, O.A. & McKinney, W.R. 1994 Conservative, high-order numerical schemes for the generalized Korteweg-de Vries equation. To appear in *Philos. Trans. Royal Soc. London A.*

Bona, J.L. & Luo, L. 1993 Decay of solutions to nonlinear, dispersive wave equations. *Differential & Int. Equations* **6**, 961–980.

Bona, J.L., Pritchard, W.G. & Scott, L.R. 1981 An evaluation of a model equation for water waves. *Philos. Trans. Royal Soc. London A* **302**, 457–510.

Bona, J.L., Promislow, K. & Wayne, G. 1994 On the asymptotic behavior of solutions to nonlinear, dispersive, dissipative wave equations. To appear in *J. Math. & Comp.*

Bona, J.L., Rajopadhye, S. & Schonbek, M.E. 1994 Models for propagation of bores I. Two-dimensional theory. *Differential & Int. Equations* **7**, 699–734.

Bona, J.L. & Schonbek, M.E. 1985 Travelling-wave solutions to the Korteweg-de Vries-Burgers equation. *Proc. Royal Soc. Edinburgh* **101A**, 207–226.

Bona, J.L. & Sciálom, M. 1993 The effect of change in the nonlinearity and the dispersion relation on model equations for long waves. To appear in *Canadian J. Appl. Math.*

Bona, J.L. & Smith, R. 1975 The initial-value problem for the Korteweg-de Vries equation. *Philos. Trans. Royal Soc. London A* **278**, 555–604.

Bona, J.L., Souganidis, P.E. & Strauss, W.A. 1987 Stability and instability of solitary waves of KdV type. *Proc. Royal Soc. London A* **411**, 395–412.

Bourgain, J. 1993 Fourier transform restriction phenomena for certain lattice subsets

and applications to non-linear evolution equations. Preprint.

Dix, D.B. 1992 The dissipation of nonlinear dispersive waves: The case of asymptotically weak nonlinearity. *Comm. P.D.E.* **17**, 1665–1693.

Foias, C. & Saut, J.-C. 1984 Asymptotic behavior, as $t \to +\infty$ of solutions of Navier-Stokes equations and nonlinear spectral manifolds. *Indiana Univ. Math. J.* **33**, 459–477.

Grad, H. & Hu, P.N. 1967 Unified shock profile in a plasma. *Phys. Fluids* **10**, 2596–2602.

Jeffrey, A. & Kakutani, T. 1972 Weak nonlinear dispersive waves: a discussion centered around the Korteweg-de Vries equations. *SIAM Rev.* **14**, 582–643.

Johnson, R.S. 1970 A nonlinear equation incorporating damping and dispersion. *J. Fluid Mech.* **42**, 42–60.

Karakashian, O.A. & McKinney, W.R. 1990 On optimal high order in time approximations for the Korteweg-de Vries equation. *Math. Comp.* **55**, 473–496.

Karakashian, O.A. & McKinney, W.R. 1994 On the approximation of solutions of the generalized Korteweg-de Vries-Burgers equation. Submitted.

Kato, T. 1975 Quasilinear equations of evolution with applications to partial differential equations. *Lecture Notes in Math.* **448**, 25–70.

Kato, T. 1979 On the Korteweg-de Vries equation. *Manuscripta Math.* **28**, 89–99.

Kato, T. 1983 On the Cauchy problem for the (generalized) Korteweg-de Vries equation. *Studies in Appl. Math., Advances in Mathematics Supplementary Studies*, Academic Press: New York, **8**, 93–130.

Pego, R.L. 1985 Remarks on the stability of shock profiles for conservation laws with dissipation. *Trans. American Math. Soc.* **291**, 353–361.

Pego, R.L. & Weinstein, M.I. 1992 Eigenvalues, and instabilities of solitary waves. *Philos. Trans. Royal Soc. London A* **340**, 47–94.

Schechter, E. 1978 Well-behaved evolutions and the Trotter product formulas. *Ph.D. Thesis*, University of Chicago.

Scott, A.C., Chu, F.Y.F. & McLaughlin, D.W. 1973 The soliton: A new concept in applied science. *Proc. IEEE* **61**, 1443–1483.

Strauss, W.A. 1974 Dispersion of low-energy waves for two conservative equations. *Arch. Rational Mech. Anal.* **55**, 86–92.

Zhang, B.-Y. 1993 Remarks on Cauchy problem of the Korteweg-de Vries equation on a periodic domain. Preprint.

Zhang, L. 1994 Decay of solutions of generalized Benjamin-Bona-Mahony equations. To appear.